SMHI
Hydrology
No 86, 2001

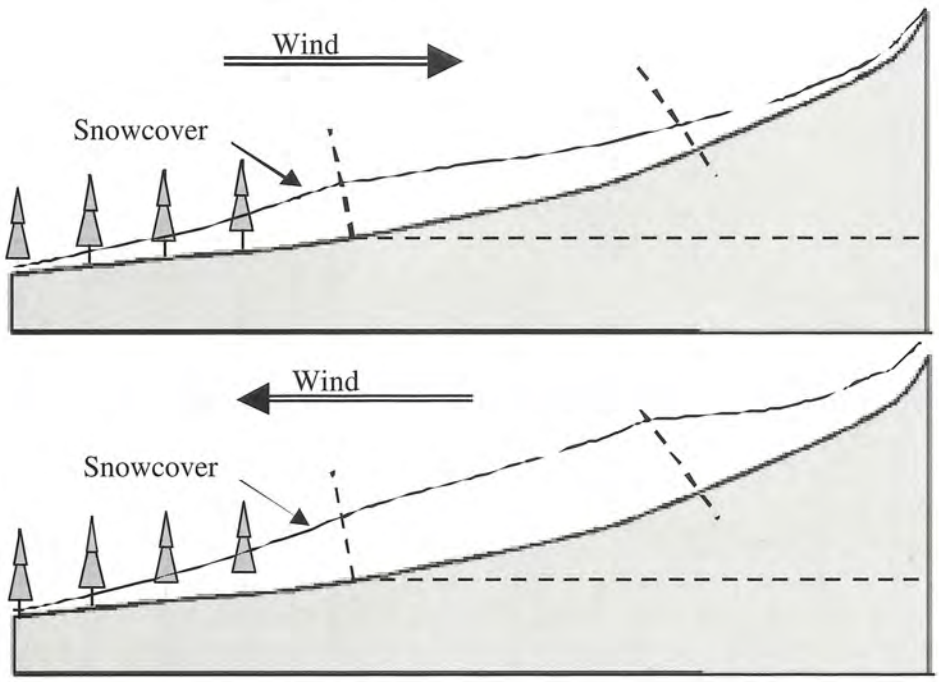

Snow distribution in a mountainous region. A remote sensing study.

Josef Källgården

Hydrology
No 86, 2001

Snow distribution in a mountainous region. A remote sensing study.

Josef Källgården

PREFACE

This report is the result of a Master Thesis Work done within the programme Aquatic and Environmental Engineering, Uppsala University, Sweden. The Swedish Meteorological and Meteorological Institute (SMHI) has financed this work. Furthermore, SMHI has provided both data for the investigation and supervision of the work.

Josef Källgården
Uppsala, March 2001

SUMMARY

This Master Thesis Work aimed to investigate snow distribution in a mountainous region in Sweden. The analyses focused on understanding the processes causing the distribution. It resulted in a suggested approach for a distributed snow model.

Snow cover was taken from remote sensing data and its distribution was analysed by means of a GIS (Geographical Information System). Snow Covered Area (SCA) was found to increase almost linearly with altitude. The increase above the timber line was found to be more gentle than below due to the redistribution of snow by wind. At some specific altitudes with certain topographic characteristics deviations from the increasing pattern were found. Those deviations could be explained by the effect of slope angles and slope aspects. Both slope angle and slope aspect affects the conditions for wind and solar radiation, which in turn affect the snow distribution. Snow is redistributed by wind from regions with high wind speed to regions with lower wind speed, i.e. from windward sides to leeward sides. Solar radiation causes snow to melt faster in slopes facing the sun.

An approach for a distributed snow model was suggested based upon the results from the analyses of snow distribution. The model is of a degree-day type and distributed in a grid-mesh. For each grid-cell correction is made for both accumulation and ablation with respect to altitude, slope aspect and slope angle.

CONTENTS

1 INTRODUCTION

1.1 BACKGROUND

The spatial distribution of snow is of importance in several hydrological and climatological processes. Today, one of the main climatological issues is the fundamental question if there is a climate change ongoing and if so, what the effects are? Several projects aim to model the climate and different climate scenarios for the future. For these simulations the snowcover is of major importance because of its high albedo and thus its high ability to reflect incoming solar radiation. A model that considers the spatial distribution of snow would be very useful when trying to simulate different climate change scenarios (Cline et al. 1998). Furthermore, a spatially distributed model would enable the use of spatially distributed input data, e.g. from satellite images. Runoff forecasts would be improved if models were updated in real-time, from e.g. satellite images (Kirschbaum 1998). Improving the forecasts is a major issue for e.g. the hydro-power companies for security and economical reasons.

Also within other sciences, a spatially distributed snowmelt model would be useful. Better spatial estimate of snowmelt would be helpful for forest harvesting, since the surface runoff may cause loss of nutrients (Ohta 1994). Furthermore, the distribution of snow in arctic tundra regions is of high importance for the survival of different plant and animal communities (Liston & Sturm 1998).

High-resolution satellite imagery is a useful tool for studying the snow distribution over large areas. According to Elder et al. (1991) a digital elevation model combined with a GIS (Geographical Information System) is an ideal tool for obtaining spatial topographic information about an area. Furthermore, remote sensing data and GIS are, according to Baumgartner & Apfl (1997), fundamental parts of several hydrological applications and they should more often be used by hydrologists. Especially information about snowcover has been obtained by various remote sensing techniques, see for instance Brandt & Bergström (1984), Sand & Bruland (1998), Rango & Martinec (1997) and Kuittinen (1989). In particular the satellite images have been widely used for obtaining information about snow distribution (Rango 1993). Furthermore, Cline et al. (1998) have concluded that remote sensing in combination with modelling could be used for water supply forecasting.

1.2 OBJECTIVES

This Mater Thesis Work is a pilot-study for a coming project at SMHI (Swedish Meteorological and Hydrological Institute) involving the construction of snow maps by combining remote sensing data and modelling. Therefore, the overall objective of this work is to provide information about snow distribution in mountainous areas, and the specific objectives are:

1. From remote sensing data investigate spatial distribution of snow in a mountainous region in Sweden and find the most important factors that affect the distribution
2. Propose a modelling approach that considers the spatial distribution of snow, with data demands that can be met in most Scandinavian catchments

2 THEORY

2.1 FACTORS AFFECTING SPATIAL SNOW DISTRIBUTION

The spatial distribution of snow is affected by several processes governing snow accumulation and ablation. To describe all factors affecting all processes at any place and any time is insurmountable even for small areas. Therefore, it is desirable to find the most important factors and a relevant scale on which these have unique values. Having done that, it would be possible to observe a specific area and from its characteristics give an estimate of the snowcover.

Blöschl et al. (1991a) and Elder et al. (1991) point out that the physical properties of the snow pack, e.g. water equivalent, depth, density and temperature, have temporal and spatial variations. These properties depend, among other things, on altitude, slope angle (shortly referred to as slope), slope aspect (shortly aspect) and solar radiance. Hence, the snow distribution of a specific area can be explained by its topography and by radiation. Observations indicate that some parameters are more important than others, and it might thus be possible to describe spatial snow distribution based on some generalisations concerning topography and solar radiation.

According to Male & Granger (1981) the energy fluxes caused by radiation and turbulence over a snow surface can not directly be linked to the altitude, although to other factors such as topography. An interpretation of this is that elevation above ocean itself does not govern energy fluxes but instead the topography, which includes information about slopes and surrounding terrain.

From the reasoning above, accumulation and ablation processes seem to be highly affected by topography. Therefore it is reasonable to use topographic information for describing spatial snow distribution. How the topographic factors affect the distribution of snow is presented below.

2.1.1 Precipitation

Precipitation normally increases with altitude, resulting in more snow at high elevations. In general, there is more precipitation over a slope that is facing the wind, i.e. the slope aspect is the same as the wind direction. The secondary effect of more precipitation over a slope facing the wind is that the gradient of increasing precipitation with altitude is mostly higher on the windward side of a mountain than on the leeward side (Barry 1981). For some areas there is also a difference in precipitation with geographical position due to orographic effects. If for example an area of quite similar topography has winds carrying humid air mainly from the west, the precipitation tends to decrease towards east in the area.

2.1.2 Wind

According to Barry (1981), the wind speed, especially when measuring in air masses quite undisturbed from topography, increases with height above ocean. The higher air masses are relatively undisturbed from ground but to a huge extent affected by global air circulation. This means that for single high mountain peaks, which are isolated from other topographic obstacles, the wind speed most often increases considerably with

altitude. Apart from altitude, Barry (1981) points out that the wind is further affected by the topography – mainly by two different processes: (1) compression of air mass which causes increased wind speed to maintain the mass and energy balance, (2) friction between air and ground which causes decreased wind speed due to the energy loss. These two processes often counteract and depending on the situation the result differs, the wind speed may increase, decrease or stay unchanged. In practice, the topographic effects on wind usually cause wind speed to be higher on the windward sides of a mountain than on the leeward side. This is a consequence of the compression of air on the windward side and a sudden expansion of the compressed air on the leeward side. The sudden expansion that comes up after the air passes the mountain top also causes, except for lower wind speed, turbulence and circular motions of air. Topography also gives rise to other wind phenomena such as fall winds caused by cool air falling down from high altitudes replacing the relatively warmer air masses at lower altitudes, thereby causing winds directed downwards along mountain sides. Thus, according to Barry (1981) wind speed is affected by both altitude and topography and the greatest variations in wind speed is caused by topography, in some cases to such extent that wind speed near ground may be even higher than up in the free air mass.

Male (1980) and Barry (1981) both presents how snow is transported by wind, a phenomena normally referred to as snowdrift. The zones where the drifting snow accumulates are often named snowdrifts. The ability of wind to transport snow is in many ways similar to how water transports particles in a river or creek. The transport is an effect of the shear stress from the moving media acting on the media to be transported. Snowdrift is divided into two transport mechanisms by Male (1980), namely *saltation* and *suspension*. Barry (1981) includes a third mechanism into the concept of snowdrift; *creep*. The three transport mechanisms can be defined as follows:

1. *creep*, snow particles are rolling along the surface without loosing contact with it
2. *saltation*, when the shear stress from wind acting on the surface is higher than a certain threshold value, snow particles are lifted up in air (up to ~1 metre) and is carried by the wind some distance before it returns to the surface
3. *suspension*, the snow particles are kept in suspension in the air mass when the vertical velocity in the turbulent eddies of wind is higher than the fall velocity of the particles

The efficiency of the three transport mechanisms is depending on the physical properties of the snow as e.g. particle size and density of particles. Even though it is hard to quantify snowdrift, some general estimates can be made. Creep is assumed to be the least important mechanism in snowdrift and is valid for only 10 % of the drift caused by saltation. The lower wind speed limit when saltation can occur is from 1.9 to 10.5 m/s (at 10 m above surface). Suspension is the dominating mechanism in snowdrift and it normally starts when wind speed (at 10 m above surface) is 4 to 12 m/s. When wind speed reaches 15 m/s or more, suspension is the only dominant mechanism. Male (1980) gives a few values of calculated and measured snowdrifts. When wind speed is 5 m/s, at 1 m above surface, the drift rate is 0.3 – 1.0 g/ms (over a unit width perpendicular to the wind) and if the wind speed is 10 m/s, at 1 m above ground, the drift rate is ~10 g/ms. This means that for a 2 km wide valley, when wind is blowing along the valley with a speed of 10 m/s, at 1 m above surface, ~72 tonnes of snow is leaving the valley every hour. Obviously, snowdrift may cause substantial redistribution of snow. As mentioned, it is difficult to estimate the amount of redistributed snow. Nevertheless, Föhn & Meister (1983) have found that the accumulation on a leeward side is about twice that of a windward side, together the two sides gets as much as a flat surface.

Bergström & Brandt (1984) have found from gamma-ray spectrometry that the snow water equivalent is about 200-300 mm on a windward side while a leeward side obtains 480-600 mm on the same altitude. The spots getting an increased accumulation from redistribution of snow are, according to Rawls & Jackson (1979), best identified through their slopes and aspects. They found from measurements that the average slope for surfaces with accumulation of snow from redistribution is 18.5°.

Barry (1981) remarks that the effect of wind on snow is also related to exchanges of sensible and latent energy. Higher wind speed often gives higher turbulence and therefore makes large energy exchanges possible, which causes either an increased cooling, warming or melting of the snow pack. According to Barry (1981), the increased energy exchange, in particular when snowdrift occurs, also makes the process of sublimation more favourable. When particles are held in the air they are in an ideal environment for sublimation, since (1) the whole snow particle is in direct contact with surrounding air which most often has lower water vapour pressure than the snow pack and (2) the high wind speed makes large latent energy exchanges possible. In fact, as much as 40 % of the suspended snow mass may sublimate (Jaedicke et al. 2000). From simulations of snowdrift in Alaska, Liston & Sturm (1998) have found that 9-22 % of winter precipitation can return to atmosphere by sublimation, for wind-exposed surfaces the return to atmosphere may be as much as 50 %.

2.1.3 Temperature

Barry (1981) gives a presentation of temperature situations in mountainous regions. The general condition is that temperature is decreasing with altitude, mainly due to the dry adiabatic temperature decrease. Because of the lower temperature, more precipitation in the form of snow and less melting are to be expected at higher altitudes.

2.1.4 Solar radiation

Several authors have described how to calculate the incoming solar radiation on a surface. The following is based on what is presented by Male & Granger (1981) and Dubayah (1992). The solar radiation that reaches a surface can be divided into three components: (1) direct radiation, (2) diffuse radiation and (3) reflected radiation. The direct radiation is solar radiation that comes directly from sun. Diffuse radiation is solar radiation that has been reflected and/or scattered from sky. Reflected radiation is the solar radiation that is reflected from surrounding terrain. The amount of solar radiation reaching a surface depends on several factors. Among the most important are the angle between surface and sun, sky conditions, length of atmosphere that solar radiation passes on its way to surface and terrain surrounding the surface of interest.

Expressions for evaluation of direct solar radiation, mostly based on principles by Garnier & Ohmura (1968), have been presented by several authors. Several authors, there among Dozier (1980), Josefsson (1985), Dubayah (1992), Ohta (1994), Dubayah & Rich (1995) and Hock (1999), have suggested improvements and simplifications to these theories. A simple complete expression for calculating direct solar radiation reaching a surface is presented by equation (1) from Dubayah (1992) with complementary equation (2) from Hock (1999).

$$I_{dir} = I_0 \cdot \cos\theta \cdot \exp\left(-\tau_0 / \cos\theta_0\right) \qquad (1)$$

$$\cos\theta = \cos\theta_0 \cdot \cos S + \sin\theta_0 \cdot \sin S \cdot \cos(D - \alpha) \qquad (2)$$

where

I_{dir} = direct solar radiation reaching the surface (Wm^{-2})
I_0 = solar constant (exoatmospheric solar irradiance) = 1368 Wm^{-2} (Lodén et al. 1971)
θ = angle between normal to the surface and sun beam
τ_0 = atmospheric optical depth (m)
θ_0 = solar zenith angle = $\pi/2$ – solar elevation
S = slope angle
D = sun azimuth (compass direction to sun)
α = slope aspect

From equations (1) and (2) follow that to maximise the direct solar radiation, the sunbeam should be normal to the surface and be as high above the horizon as possible.

Calculation of the diffuse solar radiation that reaches a surface can be done according to equation (3) from Dubayah (1992) with complementary equation (4) from Male & Granger (1981). An alternative to equation (4), which does not consider the shading effect by surrounding terrain but only the slope of the surface, is given by Josefsson (1985) in equation (5).

$$I_{dif} = (1 - V_{sky}) \cdot I_{dif0}(\tau_0) \qquad (3)$$

$$V_{sky,1} = \cos^2 H \qquad (4)$$

$$V_{sky,2} = 0.5 \cdot (1 + \cos S) \qquad (5)$$

where

I_{dif} = diffuse solar radiation reaching the surface (Wm^{-2})
V_{sky} = sky view factor, relative part of sky not seen from surface
$I_{dif0}(\tau_0)$ = diffuse solar radiation reaching a horizontal surface when optical depth is τ_0
H = average horizon angle

From equations (3) - (5), it is evident that maximum diffuse solar radiation is obtained for a horizontal surface not surrounded by any higher terrain.

In order to calculate the reflected solar radiation it may be assumed that all surrounding terrain is flat, whereby equation (6), given by Josefsson (1985) may be used.

$$I_{ref} = 0.5 \cdot (1 - \cos S) \cdot a \cdot (I_{dif,a} + I_{dir,a}) \qquad (6)$$

where

I_{ref} = reflected solar radiation reaching the surface (Wm^{-2})
a = albedo of the surrounding terrain
$I_{dif,a}$ = diffuse solar radiation reaching surrounding terrain (Wm^{-2})
$I_{dir,a}$ = direct solar radiation reaching surrounding terrain (Wm^{-2})

Maximum reflected solar radiation is obtained when a surface has large slope angle to make it as exposed to the surroundings as possible and the surroundings have a high albedo and receive a lot of radiation. In mountainous areas sloping surfaces with completely flat surroundings are not very frequent. A more realistic case is a situation with the surface on the bottom of a valley surrounded by snow covered slopes.

In mountainous areas, there are not enough actual measurements of solar radiation to estimate the spatial variation, however, Josefsson (1985) has measured solar radiation on surfaces surrounded by flat terrain in Stockholm, Sweden, during May and June. Measurements of diffuse and global radiation were done and calculations provided values for incoming direct, diffuse and reflected solar radiation for different slopes. If reflected radiation is calculated, assuming an albedo of 0.6 and the daily averages of all three components are added, the resulting relative radiation is given as illustrated in *Figure 1*. The greatest variations are due to the variations in direct solar radiation.

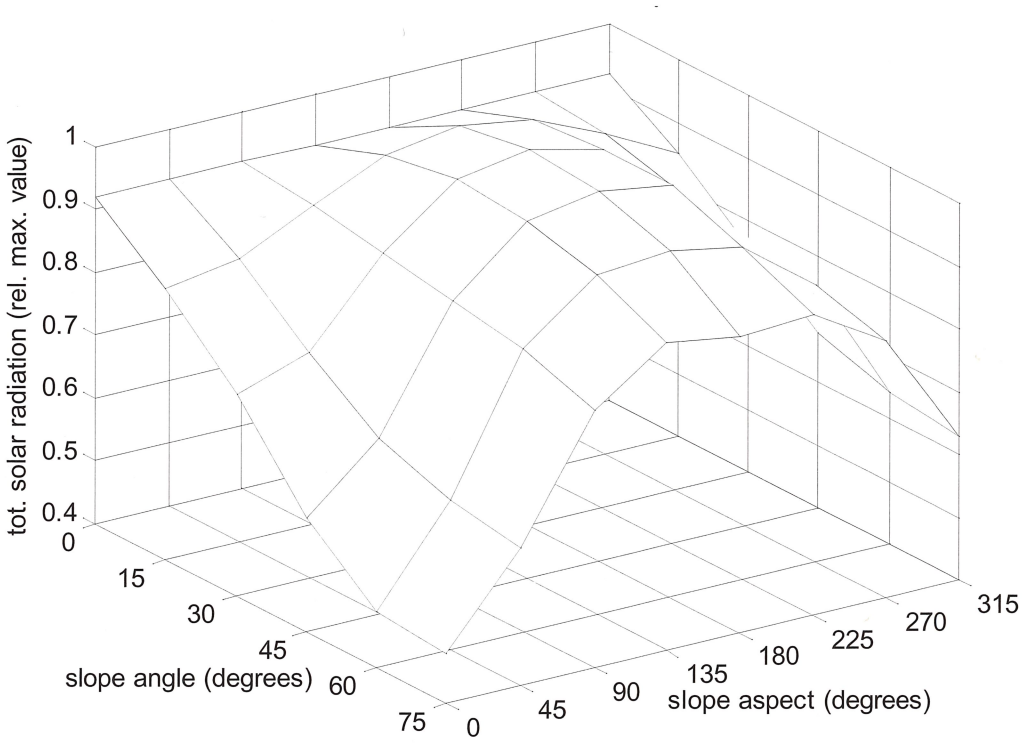

Figure 1 *The sum of direct, diffuse and reflected (albedo = 0.6) solar radiation (relative to max. value) in Stockholm May-June, 1971-1980. Slope aspect defined as zero in north and increasing clockwise. After Josefsson (1985).*

As *Figure 1* shows, maximum radiation is obtained for south-facing slopes with slope angle 30°. This means that the topographic effect on solar radiation in Stockholm, May-June, causes south-facing slopes with 30° slope angle to get the most solar radiation and north-facing slopes with 75° slope angle to get the least solar radiation. For other places on the same latitude the result is probably similar, unless the places differ in other factors that affect the result, e.g. cloudiness. For an area on a higher latitude, the differ-

ences in solar radiation for different aspects are most probably smaller since the sun is above the horizon for a longer part of the day and since its greatest elevation above horizon is lower. Another effect of the sun having a lower maximum height above horizon is that the maximum obtained solar radiation would occur on steeper slopes, e.g. 45° instead of 30°.

2.2 SPATIALLY DISTRIBUTED SNOW MODELS

As will be shown from the literature cited below, modelling of spatial snow distribution mostly focuses on the melting. Accumulation is not given much attention. Either it is estimated as extrapolated data from field measurements or simply regarded as known from intense field campaigns. As for the accumulation of snow, there are some previous projects concerning the snowdrift but they seem to be restricted by the extraordinary computer capacity needed for the simulations. Simulations have been done for relatively small areas, see for example Jaedicke et al. (2000) and Liston & Sturm (1998).

2.2.1 Methods for modelling snowmelt

Leavesley (1989) presents the two most important different ways to calculate snowmelt. The first way, which is physically most correct, is to use an energy balance which demands several physical parameters as input. The second way, the degree-day method, is of index-type only using air temperature as an input.

Energy balance

According to Male (1980) there are two approaches that can be used to calculate snowmelt from an energy balance. Either by considering energy exchanges at the snow surface, or by regarding the whole snowpack as a control volume over which fluxes and heat changes are considered. In both cases, the fluxes are of different types, mainly; shortwave radiation, longwave radiation, sensible and latent heat flux. To calculate these fluxes a number of parameters has to be known, among those; temperature in air, snow and soil, air humidity, wind speed, wind profile and cloudiness. Since wide areas that receive snow in the winter are in non-inhabited regions it is often hard to obtain all those parameters.

The degree-day method

According to Rango & Martinec (1995), the degree-day method has been used for more than 60 years and is still in use for calculating total snowmelt in drainage basins. The accuracy is satisfying for this purpose when whole basins are modelled and time steps no shorter than a week are used. Still, the method is often used with a time step of 1 hour. However, the method is not perfectly suited for describing the spatial distribution of snow.

The degree-day method is used to calculate snowmelt with a timestep of one day in the HBV-96 model, which is the model SMHI uses. Lindström et al. (1996) provides the degree-day method used in the HBV-model:

$$MELT = CFMAX \cdot (T - TT) \qquad (7)$$

where

MELT	= snowmelt (mm/time step)
CFMAX	= degree-day factor (mm H_2O/(degree timestep))
TT	= threshold temperature
T	= air temperature

The only meteorological input in this method is air temperature, which does not give a correct picture of reality in terms of snowmelt. Nevertheless, the method is said to include other processes that are explicitly written in an energy balance, by adjustments of CFMAX and TT. CFMAX is often assumed to be a constant, which according to Rango & Martinec (1995) is inaccurate. They suggest that CFMAX should increase during the melt period. According to Leavesley (1989), CFMAX should be allowed to vary spatially as well, due to differences in solar radiation, land cover and altitude.

Lindström et al. (1996) report that work has been done for the HBV-96 model to let the degree-day method develop towards an energy balance but this did not result in better results concerning the simulation of river runoff. Furthermore, experiments where CFMAX is varied have been performed in order to increase the predictive ability of the HBV-96 model. CFMAX has then been allowed to vary with time, precipitation and wind speed but none of these attempts lead to better results. Although, depending on the land cover, CFMAX is given different values in the lumped HBV-96 model depending on whether the area is forested or not (Lindström et al. 1996).

Extended degree-day method

According to Rango & Martinec (1995), the accuracy of the degree-day method can be increased for short time-steps and small areas if a radiation component is added to the method. The extended degree-day method is then given by:

$$MELT = CFMAX \cdot (T - TT) + M_R \cdot (1 - a) - G \qquad (8)$$

where

M_R	= global radiation converted to melting (mm H_2O/timestep)
a	= albedo
G	= net outgoing longwave radiation converted to melting (mm H_2O/timestep)

According to Martinec (1989), another approach is to use:

$$MELT = CFMAX \cdot (T - TT) + M_Q \cdot R_N \qquad (9)$$

where

M_Q	= melt factor for net radiation (mm H_2O/(timestep (W/m^2)))
R_N	= net radiation (W/m^2)

The resolution increases, both temporally and spatially, if radiation is added to the degree-day method according to equation 8 or equation 9. The method demands one or two extra components as input though. Another approach is presented by Hock (1999), who combines the potential direct solar radiation with temperature according to:

$$MELT = (CFMAX + K \cdot I) \cdot (T - TT) \qquad (10)$$

where

K = radiation coefficient (mm H_2O/(timestep (W/m^2)))
I = potential direct solar radiation (W/m^2)

When using this method with a timestep of one hour, Hock (1999) obtained satisfactory modelling results concerning the temporal and spatial variations of melt on the glacier Storglaciären in Sweden.

2.2.2 Models including the spatial distribution of snow

There are several models that concern the spatial distribution of snow. Cline et al. (1998) calculated the energy balance in each cell of a grid-mesh. The radiation input was estimated from topographical data and both shadowing as well as reflecting effects of the terrain were considered. Another spatially distributed model is presented by Ohta (1994), who used the energy balance and calculated solar radiation from topographical data. Energy balance was also used by Blöschl et al. (1991b) to model spatial snowmelt. The shortwave radiation was then calculated while excluding all shading effects and assuming all reflecting radiation was from a flat surrounding terrain. According to the modelling results, the radiation assumptions done by Blöschl et al. (1991b) are realistic.

Several distributed models use the degree-day approach as well. Among those is a model presented by Kirschbaum (1998), in which the melt factor is varied temporally and spatially. The time dependent variation in the melt factor is a discrete sinusoidal function with specific values for each month and a maximum in June. Spatial variation of the melt factor is calculated from topography as to reflect the solar radiation conditions a clear mid-summer day. The model has been implemented for a Norwegian mountainous catchment without forest and an average altitude of 1100 m. This model gave better predictions of maximum SWE (Snow Water Equivalent) in the catchment than a lumped HBV model. Hock (1999) used the degree-day method as given in equation 10 to model spatial snow melt, in this case for snow on a glacier, Storglaciären, situated 67°55'N 18°35'E at altitude 1120-1730 m. The potential direct solar radiation was calculated from a digital elevation map and the timestep was one hour. The results showed correct variations in snowmelt, both temporally and spatially.

3 MATERIAL AND METHODS

3.1 MATERIAL

3.1.1 Snow distribution from satellite images

The spatial snow distribution in an area of approximately 5000 km^2 was obtained from processed satellite remote sensing data available at SMHI (see Rott et al. 2000). The distribution was given for the same area at four occasions, 1992/06/02, 1992/06/09, 1992/06/25 and 1996/06/04. According to Klein et al. (1998) it is difficult to distinguish snow cover from no snow cover in forests due to the shading effect of the vegetation. On glaciers and lakes there may be bubbly ice that appears white and thus incorrectly might be classified as snow. Thereby, the classification of snow and not snow in forests, on glaciers and lakes is of comparatively low quality. The processed data are in a gridded form, i.e. the area over which snow cover is examined is divided into cells by a regular grid-mesh. Each grid-cell (also referred to as pixel) represents a square of 30 by 30 metres and is associated with an attribute which is "1" if the square is covered with snow or "0" if the square does not have snow. The grid-mesh may also be regarded as a matrix where each element has value 1 or 0 and represents a 30 metre square in the terrain. In this study, the data were analysed in a GIS (Geographical Information System) - a computer-based system for acquiring, processing, analysing, storing and presenting geographical data (Malmström & Wellving 1995), and also with help from Matlab - a language for computing, that is suited for handling matrices.

The analyses were done focusing on Snow Covered Area (hereafter referred to as SCA). The SCA is not directly proportional to the amount of snow, or Snow Water Equivalent (hereafter referred to as SWE). Yet, there are investigations that show a positive correlation between SCA and SWE, see for example Kuittinen (1989) who achieved a positive correlation coefficient of 0.89.

3.1.2 Investigated area

The area of study is a mountainous region in northern Sweden. The area has the shape of a rectangle with lower left corner at X1565000 Y7430000 and upper right corner at X1640000 Y7500110, given in Swedish national co-ordinates (RT90), where X denotes the eastern position and Y the northern. In latitude and longitude the lower left corner is approximately 66°50'N 17°15'E.

The area includes the National Park of Sarek and is east of the major water divide that defines the Baltic Sea drainage basin. The area includes several high peaks, great areas above the timberline, several glaciers and lakes, wetlands, forest and open ground, (*Figure 2* and *Figure 3*).

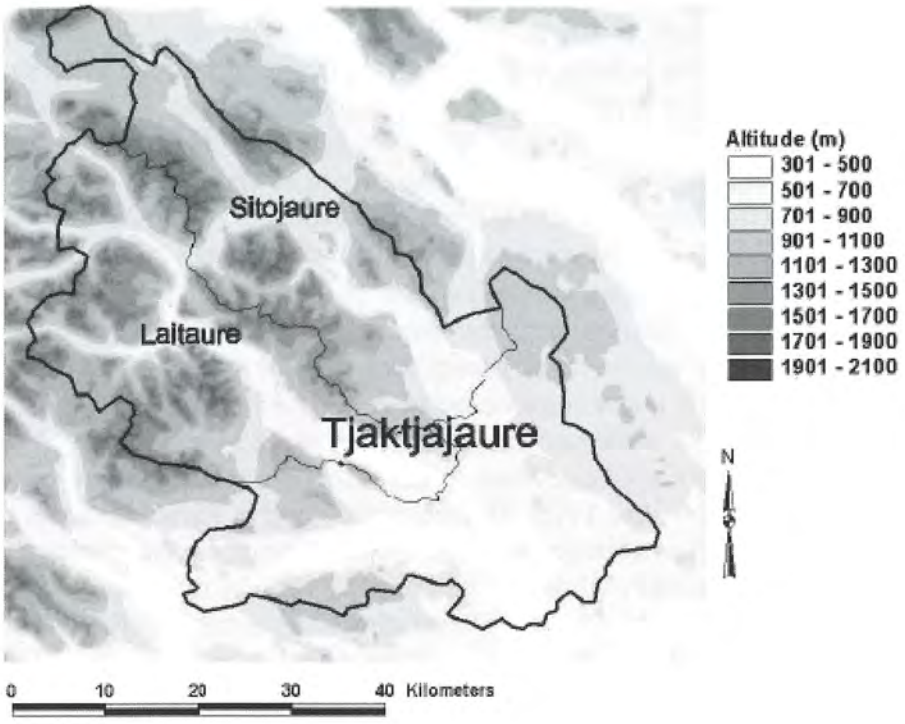

Figure 2 *Investigated area. Altitude and the main catchment Tjaktjajaure with subcatchments Laitaure and Sitojaure are shown.*

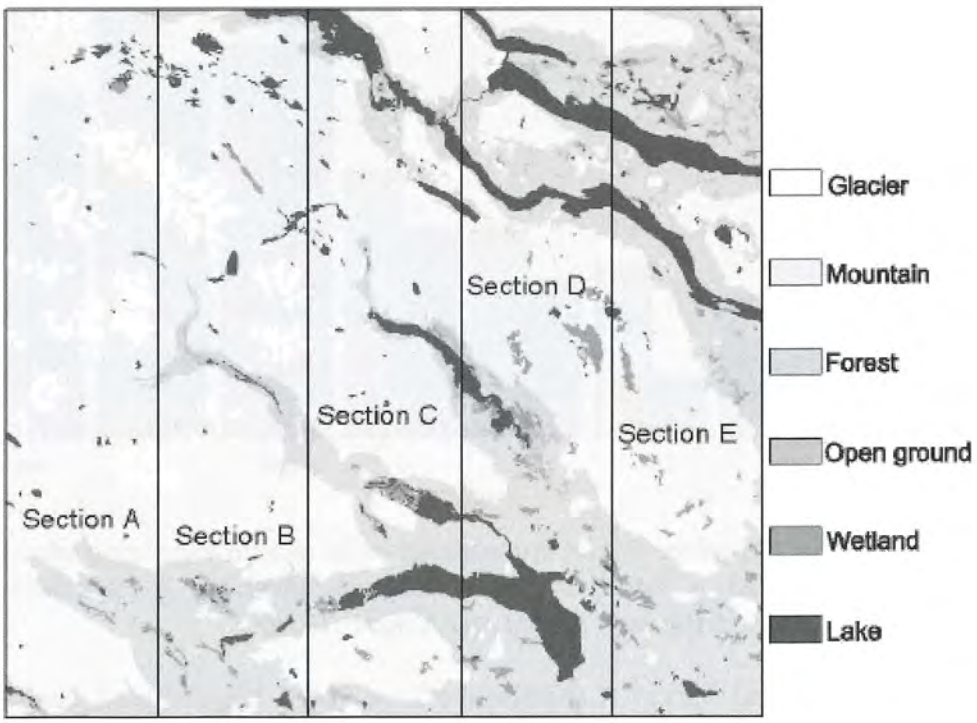

Figure 3 *Land cover within the investigated area. Five sections used as sub-divisions for limiting the area for analyses are also marked (sections A-E).*

The area receives a lot of precipitation, especially during winter. Furthermore, there is a large gradient in precipitation which is decreasing from west to east (Bergström & Brandt 1984). The whole area is within the global westwind belt which means that the geostrophic winds are mainly from west (see for instance Palmén & Newton 1969). Data on geostrophic wind, calculated at SMHI from synoptic observations, were also available for the investigated area (*Figure 4*). The data of interest for this study were a series of geostrophic wind directions, every third hour from 1981 to 1998, calculated for the position 67.5° N 17.5° E and assumed to be valid for the "square" defined by integer latitudes and longitudes, (i.e. within the area 67-68° N 17-18° E). There are also elder data of wind direction observations from the area of interest. During the years 1914-1916 wind directions were measured at Pårtetjåkkå (*Figure 4*), which is a mountain peak situated within the area, under supervision of Axel Hamberg (Hamberg & Jönsson 1933 and Köhler 1939). The measurements were done at 1834 m altitude at position X1579000 Y7452500, 5.8 m above ground. Wind direction was observed every hour during the period July 1914 – June 1916. The measured wind at Pårtetjåkkå and the calculated geostrophic wind shows similar patterns. Southwestern winds dominate among the measurements at Pårtetjåkkå, while the geostrophic wind is dominated by western winds. This is consistent with the theory of wind directions turning to the left at lower altitudes (at northern hemisphere) due to the coriolis effect (see for instance Liljequist 1962).

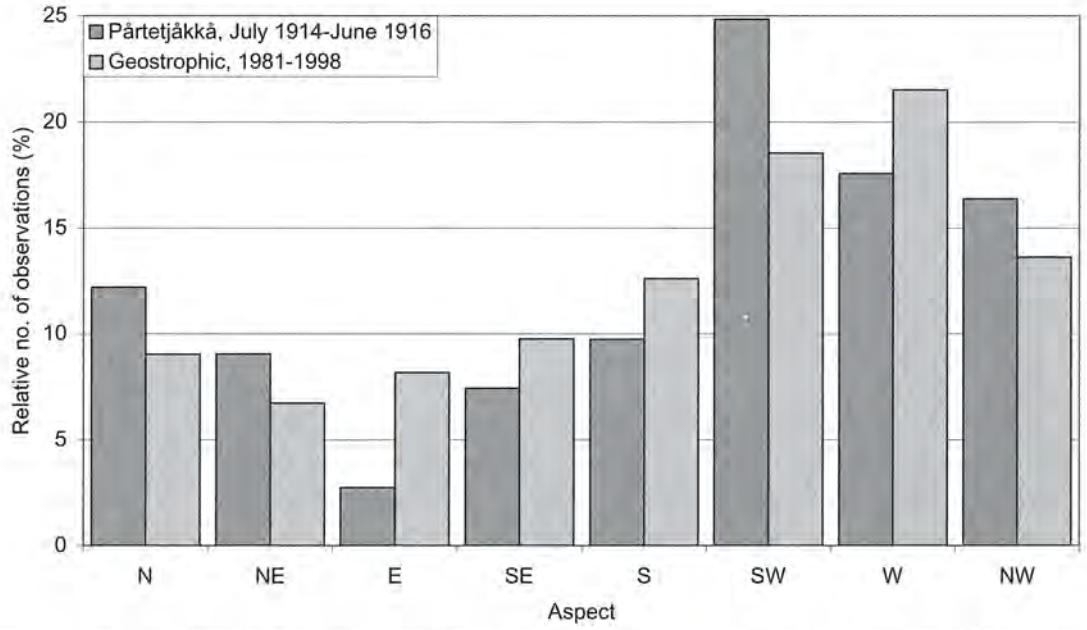

Figure 4 *Wind directions in the investigated area, geostrophic wind direction as calculated at SMHI, and measured wind direction at Pårtetjåkkå after Hamberg & Jönsson (1933) and Köhler (1939).*

From the Swedish Land Survey (Lantmäteriverket), SMHI has obtained databases including information about altitude and land cover with a resolution of 50 m. These databases were used in this study and the resolutions were recalculated to 30 m to facilitate the comparison with the snow distribution data. The recalculation was done by the GIS-application ArcInfo Grid. Thereby databases of the same format as the snow distribution data were obtained; land cover as a grid-mesh with each cell having a number

corresponding to the type of ground for that 30-metre square and for the altitude database as a grid-mesh with each cell having a value corresponding to the altitude. From the altitude grid-mesh, calculations of slopes and aspects were done by the GIS-application ArcInfo Grid. The resulting aspect is given as 0° when the slope is facing north and increasing clockwise. These calculations resulted in four grid-meshes with information about the area; land cover, altitude, slope and aspect, all with resolution 30 m. Regarded as matrices the grid-meshes had 2337 rows and 2500 columns each.

3.1.3 Topography and land use

From *Table 1* it is clear that the western parts of the investigated area is on a higher altitude and also have greater variations in altitude. The correlation coefficient between average altitude and eastern co-ordinate (*Figure 5*) is –0.97 and the correlation between average altitude and relative area of forests is –0.94.

Table 1 *Altitude characteristics in the investigated area*

	Section A	B	C	D	E	whole area
Average altitude (m)	1093	988	859	664	639	849
Median altitude (m)	1083	923	839	635	614	800
Min altitude (m)	357	327	374	301	366	301
Max altitude (m)	1999	2058	1807	1411	1093	2058
Standard deviation (m)	315	332	286	197	162	321

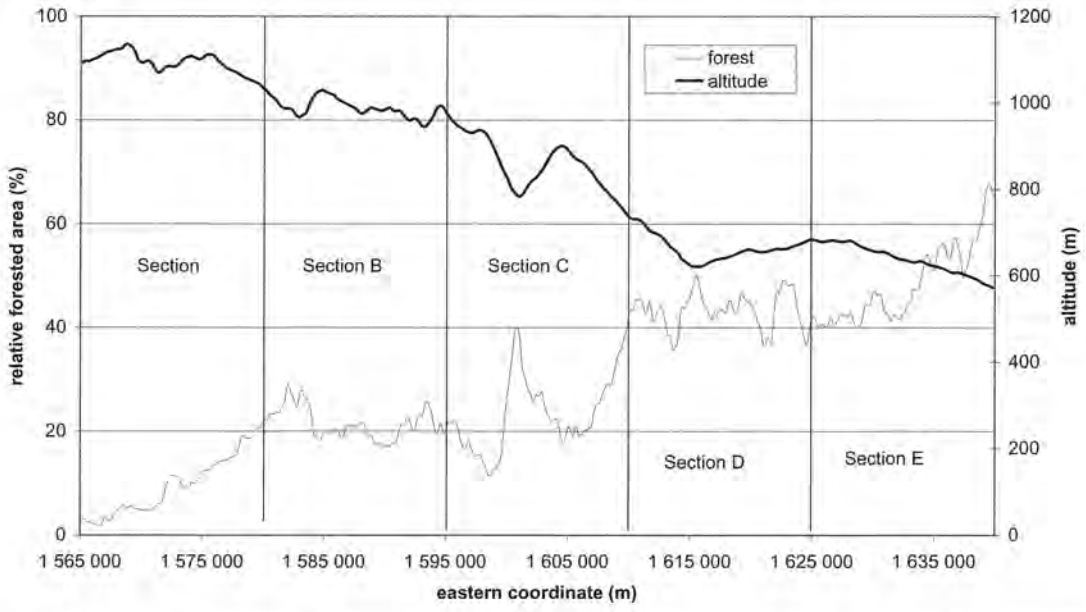

Figure 5 *Average altitude and relative forested area, variations with eastern co-ordinate, 240 m running average.*

The relative areas of flat surfaces are increasing with eastern and northern co-ordinates. The northeastern, northern and northwestern aspects are decreasing with eastern co-ordinate and increasing with northern co-ordinate while the opposite is valid for south-

western aspects (*Table 2*). What is seen in *Table 2* is to some extent a result of the area having high peaks in the centre and surrounding lower regions.

Table 2 *Correlation coefficients between aspects and co-ordinates*

	Flat	N	NE	E	SE	S	SW	W	NW
East	0.71	-0.38	-0.15	0.01	-0.19	-0.16	0.11	0.02	-0.40
North	0.29	0.35	0.24	-0.16	-0.34	-0.31	-0.32	-0.06	0.14

As a result of the great valleys in the area (*Figure 2*), the aspects northeast, south and southwest are the most common aspects (*Table 3*). Since those valleys are U-shaped, their sides are steeper higher up and accordingly the relative areas of northeastern and southwestern aspects are relatively smaller at higher altitudes (*Table 3*). The correlations in *Table 3* were calculated for section A when forest, lakes and glaciers were excluded and only for the altitude interval 730-1606 m, since the area below 730 as well as the area above 1606 m, is only accounting for 5 %. The correlations further suggest that southeastern and northwestern aspects more common at higher altitudes.

Table 3 *Aspect characteristics, relative area (%)*

	Section A	B	C	D	E	whole area	correlation with altitude
Flat	1.4	3.4	8.4	14.1	8.7	7.2	-0.21
N	14.8	14.5	12.7	9.7	11.7	12,7	-0.37
NE	16.6	14.6	15.8	11.7	16.0	14.9	-0.81
E	10.6	10.6	11.3	9.3	11.2	10.6	-0.51
SE	9.6	9.7	9.2	8.4	8.7	9.1	0.59
S	16.4	15.1	14.5	13.9	15.0	15.0	0.09
SW	13.9	14.3	13.2	15.1	14.4	14.1	-0.22
W	8.5	9.9	8.4	11.1	8.3	9.2	0.11
NW	8.2	7.8	6.5	6.7	5.9	7.0	0.82

More detailed investigations of the variation of aspects with altitude showed certain anomalies at specific elevations. This is illustrated by e.g. *Figure 6*, where the whole area (forest, lakes and glaciers excluded) has relatively large areas of flat surfaces and southeastern aspects at heights around 900 and 1200 m. At the same altitudes, the areas with the southwestern, western and northwestern aspects are relatively smaller than at lower and higher altitudes. The same patterns are found in section A and catchment Laitaure.

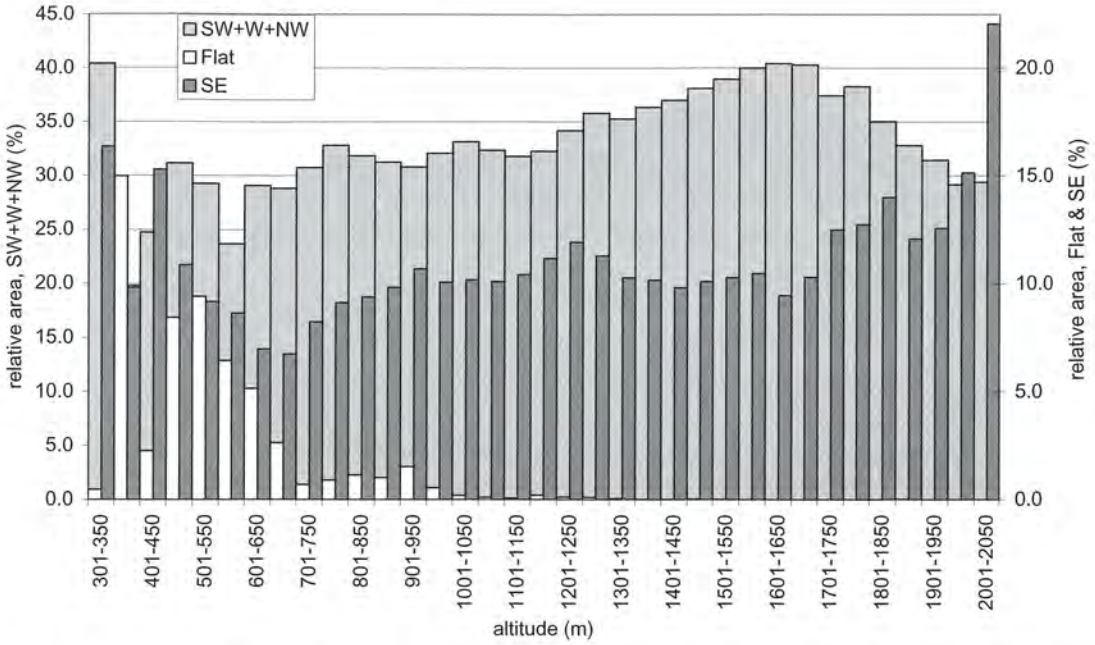

Figure 6 *Variations of flat areas, southeast aspects and the sum of southwest, west and northwest aspects with altitude. Whole area when forest, lakes and glaciers were excluded.*

The average slope for the whole area is 9.7°. *Figure 7* shows that slopes around 2.5° are the most common in the whole area. For the western parts, steeper slopes are more common and for the eastern parts more gentle slopes are more common.

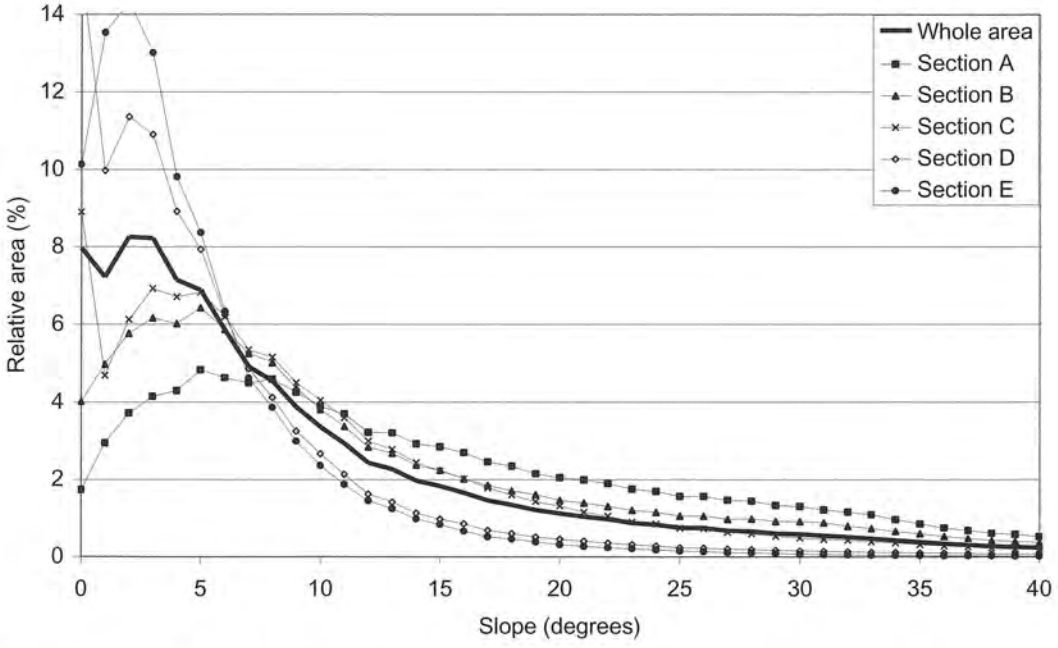

Figure 7 *Distribution of investigated area with respect to slope.*

The distributions of slopes over elevation show a clear tendency of steeper slopes being situated at higher altitudes. The most gentle slopes show some anomalies from that pattern. In *Figure 8* the distributions of slopes <20° over altitude in Laitaure are shown. Flat and gentle slopes occupy large areas at altitudes ~900 m and ~1250 m. The same patterns are found for the whole area and for section A. This is also shown by *Figure 9*, and it is evident that there are large areas of flat and gently sloping ground around 1200 m. *Figure 9* further shows that peaks above ~900 m are isolated. Therefore, it may be suspected that those peaks are more exposed to wind than the areas below ~900 m. The same is valid for ~1200 m.

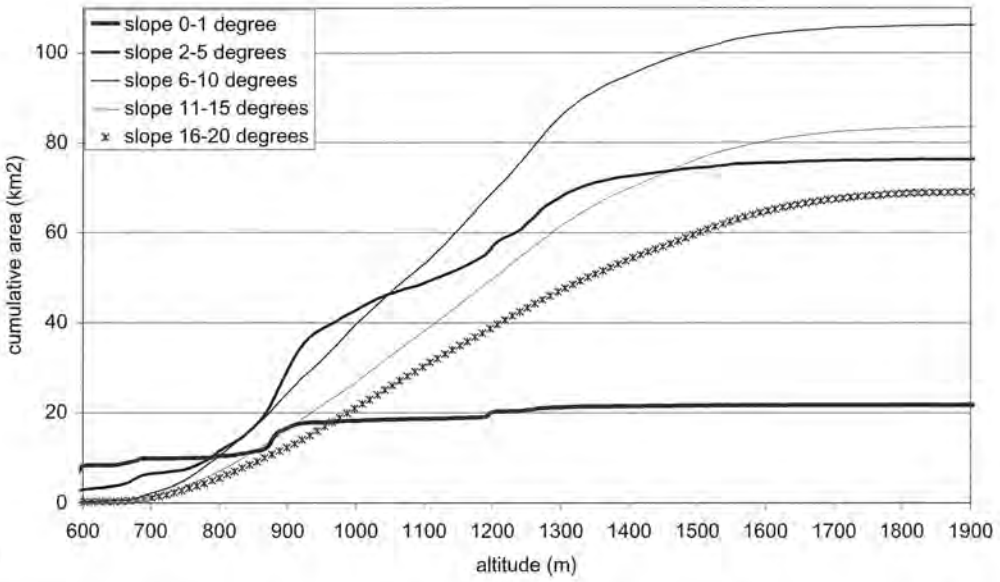

Figure 8 *Cumulative area of slopes over elevation. Laitaure, forest, glaciers and lakes are not included.*

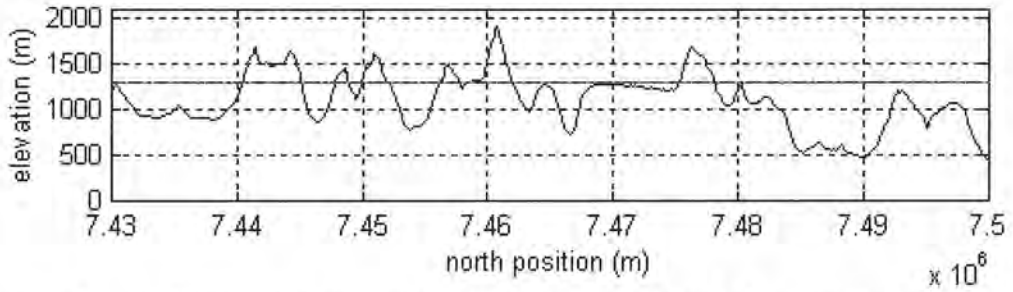

Figure 9 *Transect from south to north through whole area at eastern position 1575000 m. Altitude 1200 m is marked in the plot.*

The relative areas sloping less than 11° are decreasing with increased altitude and relative areas sloping steeper than 21° are increasing with increased altitude (*Table 4*). The coefficients and R^2-values in *Table 4* are obtained by firstly, calculating the relative areas (normalised with their maximum value) of slopes for every altitude interval of 1 m. Secondly, performing linear regressions between altitude and normalised areas for slopes.

Table 4 *Linear regression of normalised relative area of clustered slopes and altitude. Section A with forest, lakes and glaciers excluded*

Slope (degrees)	Normalised relative area is proportional to altitude with a coefficient	R^2-value for linear regression	Total area (km^2)
0-10	-0.0006	0.92	339
11-21	0.00006	0.23	252
22-32	0.0002	0.82	154
33-42	0.0002	0.72	68
43-53	0.00009	0.62	30
54-64	0.00008	0.47	6

Glaciers occur at the highest altitudes, followed by mountains (not forested). Below those are wetlands, open ground and forests and, at the lowest altitudes, lakes (*Figure 10*). Lakes and wetlands are far more common on some specific altitudes than others, for example is almost 60% of the total lake area within the interval 400-500 m. The wetlands and open grounds are 10-100 times more common at slopes <5° compared to slopes >5°.

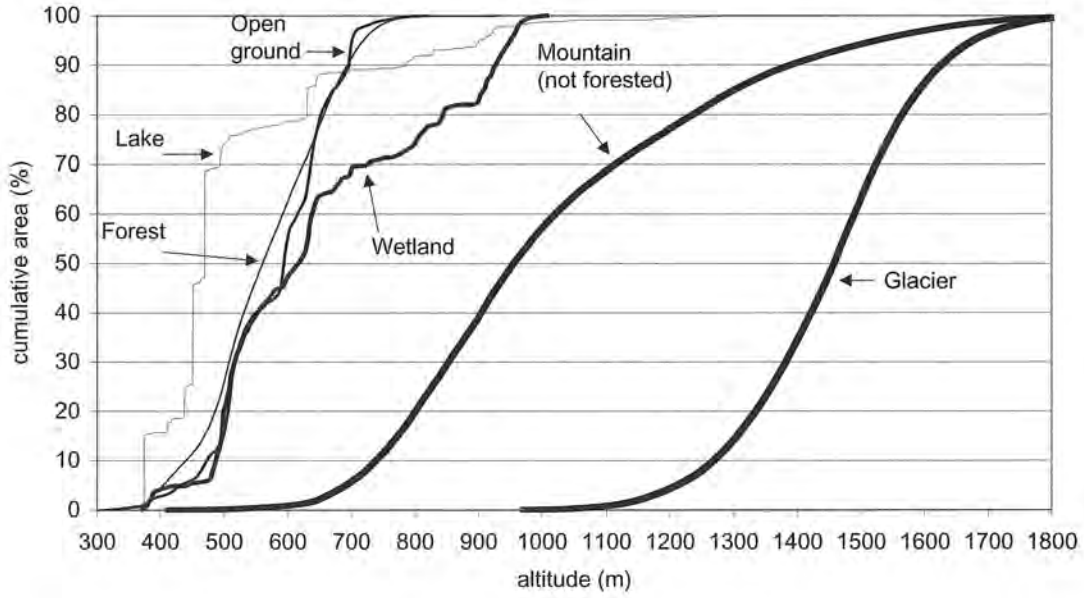

Figure 10 *Distribution of land covers for whole area with respect to altitude.*

Table 5 shows that the land covers most common at high elevations (see *Figure 10*) are less frequent in the eastern regions of the area. The opposite, i.e. frequent occurrence in the eastern regions, is valid for the land covers that are most frequent at lower altitudes.

Table 5 *Land characteristics, relative areas (%)*

Land cover	Section A	B	C	D	E	whole area
Mountain (not forested)	79.9	67.6	64.5	37.2	38.0	57.4
Forest	9.4	21.5	23.5	43.3	48.4	29.2
Lake	1.1	3.2	9.3	13.7	7.7	7.0
Glacier	8.6	5.4	0.4	0.0	0.0	2.9
Wetland	0.7	0.9	1.1	3.6	3.1	1.9
Open ground	0.2	1.3	1.2	2.2	2.8	1.5

The glaciers are mostly occuring on northeastern and eastern aspects, while the aspects with least glacier area are southwestern and western (*Figure 11*). The distribution of glaciers are closely connected to wind direction. Correlation coefficients between distribution of glaciers on aspects and wind directions are –0.86 for Pårtetjåkkå wind and –0.96 for the geostrophic wind.

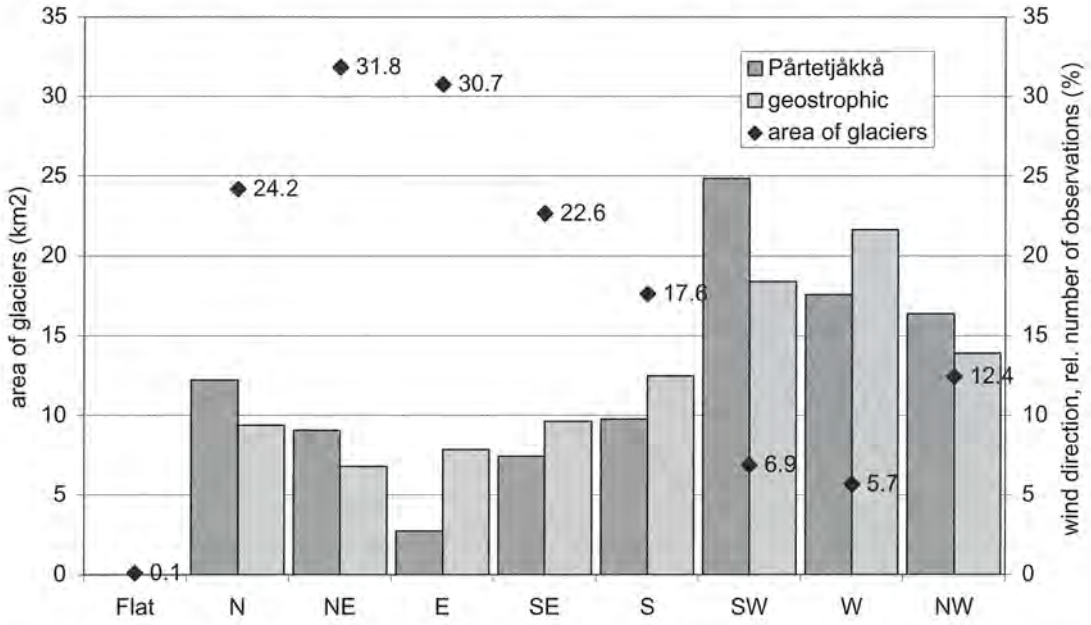

Figure 11 *Distribution of glaciers with respect to aspects in whole investigated area. Also measured wind directions at Pårtetjåkkå 1914-1916 and calculated geostrophic wind directions 1981-1998.*

The geostrophic wind is mainly westerly and measured wind directions at Pårtetjåkkå are dominated by southwestern winds (see *Figure 4* and *Figure 11*). The geostrophic wind data, also show that the winter 1991/1992 was more dominated by western winds than the average of the period 1981-1998. During the winter 1995/1996 the westerly and easterly winds were almost equally frequent. Instead, the southern winds were more frequent than the northern this particular winter.

3.2 METHODS

3.2.1 Analysing snow distribution

When performing the analyses several combinations of the available variables (see *Table 6*) were used. For most combinations the data were subdivided to represent either one of the catchments presented in *Figure 2* or any of the equally sized sections in *Figure 3*. This is reasonable since the whole area is quite large which makes it likely that there are considerable differences in unknown factors, such as precipitation. Furthermore, the land-covers glacier, forest and lake were excluded from most analyses. This was due to their relatively low quality of snow cover data, see section 3.1.1, and due to the deviant pattern of snow cover on lakes and glaciers.

Table 6 *Variables available for analyses*

Variables affecting snow distribution:	Resulting snow distributions:
Eastern position	SCA 1992/06/02
Northern position	SCA 1992/06/09
Land cover (6 classes, see *Figure 3*)	SCA 1992/06/25
Altitude (see *Figure 2*)	SCA 1996/06/04
Slope angle	
Slope aspect	
Wind direction at Pårtetjåkkå (see *Figure 4*)	
Geostrophic wind direction (see *Figure 4*)	

Since all variables (except the wind directions) were in grid-meshes covering the same area and having the same resolution, the analyses could conveniently be done by taking combinations of them with either the GIS-applications ArcView Spatial Analyst or ArcInfo Grid, or the language for computing - Matlab. For some cases, the difference in SCA between two observations 1992 was regarded as the melting and used as a resulting melt distribution. For some analyses, the variables were clustered in intervals. The most usual clusterings are presented in *Figure 12*.

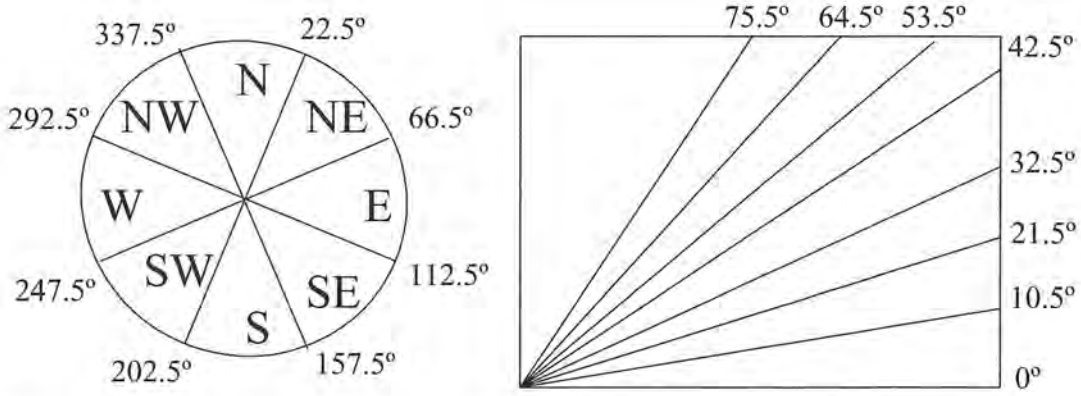

Figure 12 *Clusters for aspect and slope used in the analyses.*

The analyses were done by first looking at several plots generated from the combinations of different variables and then calculating correlation coefficients for interesting combinations.

Aspect has values that are difficult to analyse statistically directly due to the fact that 0° and 359° are as close to each other as 0° and 1°. Therefore, correlations with aspects involved were done by taking the cosine and sine of aspect. Since 0° is in north, cosine of aspect will result in a number between –1 and 1 telling to what extent the particular aspect is pointing to the north. In the same way, sine of aspect gives a number between –1 and 1 telling to what extent the aspect is pointing to the east. Hence, cosine and sine of aspects were calculated and denoted north-aspect and east-aspect.

In the previous section characteristics concerning the investigated area were presented, i.e. characteristics of and dependencies between the affecting variables. These results were important for further work with correlations between SCA and the affecting variables. Knowledge of the internal dependencies between the affecting variables made it easier to avoid incorrect conclusions from correlations between SCA and single affecting variables. As a hypothetical example, if there is a high correlation between northern position and altitude one should at a later stage be aware that a high correlation between SCA and northern position may simply be a result of SCA depending on altitude.

3.2.2 Performing resolution control of proposed modelling approach

For a model distributed in a grid-mesh, the size of grid-cells is deciding the resolution of the model. Each cell in the grid-mesh may be related to unique values such as aspect and altitude. These parameters may have certain scales where they are no longer varying spatially. Therefore, a resolution control was performed to investigate whether there is a cell-size where the difference between two cells is no longer detectable.

The control was done by continuously increasing the grid-cell size and compare cells to each other with respect to (1) aspect, or (2) snow amount calculated with respect to aspect and/or altitude. Thus, the cell values were either north-aspect, east-aspect or snow amount.

Irrespective of what the cell values were, the control was done in five tests. Each of the five tests was done as follows. First, four grid cells were distributed over the available investigated area. Then, their cell sizes were increased and finally the difference or ratio between their average values for varying cell sizes was calculated. The difference between the five tests was to distribute grid cells according to *Figure 13* in five different regions of the investigated area. Grid cell size was first 100 m and then increased in steps of 100 m.

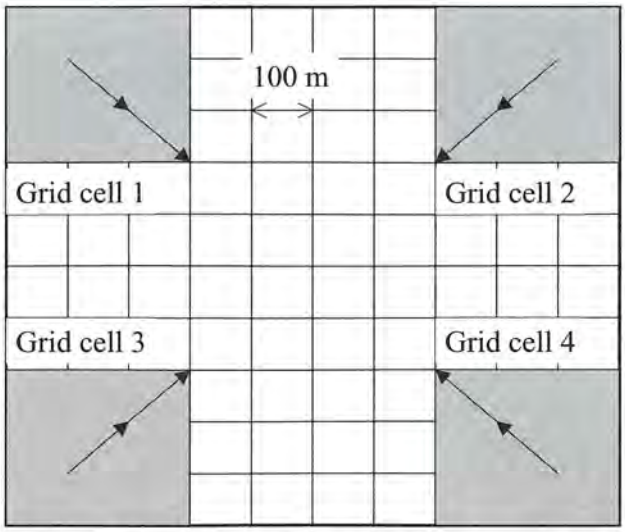

Figure 13 *Method for distributing and increasing grid cells for resolution control.*

First, a resolution control was done to investigate if there was a critical cell size where there was no difference between cells with respect to their aspect. The difference was calculated by subtracting the average north-aspect (or east-aspect) of one grid-cell with the average value of another cell. This gave the cell size at which the information about aspect would be unnecessary, since grid cells would have approximately the same average aspect.

Secondly, a resolution control was performed to investigate if there was a critical cell size where there was no difference between cells with respect to their snow amount. The differences were investigated by calculating the ratios between cells. Two alternative tests were carried out. In one of them the altitude information was completely excluded and only the variations in snow amount caused by aspect and slope were considered, in the other also the elevation dependency of precipitation and temperature was included.

4 RESULTS

4.1 EMPIRICAL SNOW DISTRIBUTION

Unless other information is given, the land-covers forest, glaciers and lakes are excluded from all the presented results.

4.1.1 Geographic distribution

The variation of SCA with eastern co-ordinate showed a high resemblance to the average altitude, see *Figure 14*. Snow melt was computed as the relative difference in SCA from 1992/06/02 to 1992/06/09 and shows the opposite pattern with high melt rates at low altitudes. For the other occasions, 1992/06/09, 1992/06/25 and 1996/06/04 the distributions of SCA were similar as in *Figure 14* but the absolute values differed.

High correlations were found between SCA/melting and eastern position and average altitude respectively (see *Table 7*). Also, high correlation between northern co-ordinate and melting was seen. The melting is the above mentioned difference in SCA and the altitude is a running average over an eastern co-ordinate interval of 240 m. When calculating the correlations for melting, the co-ordinate intervals that did not have any snow (after the melt period) were excluded. The intervals used for correlation with melting are thus eastern; 1565000 to 1613510 and northern; 7431650 to 7500080.

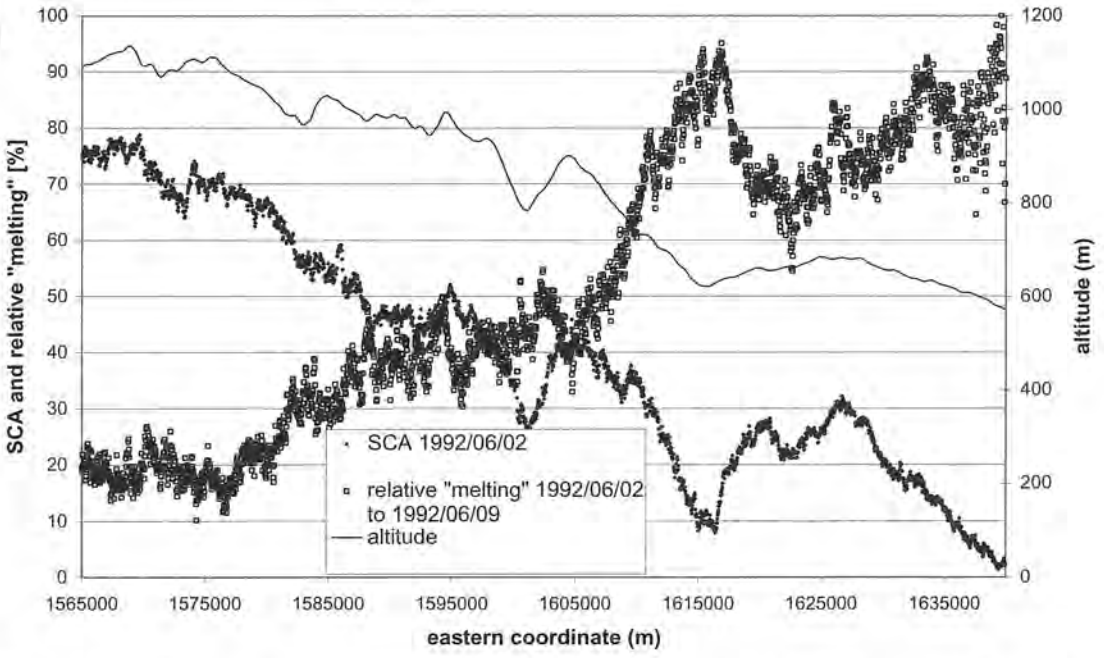

Figure 14 *Eastern distribution of SCA and melting, also a 240 m running average of altitude, whole area and all land covers.*

Table 7 *Correlation coefficients concerning geographical co-ordinates, altitude, SCA and melting. For whole area and all land covers*

	SCA 1992/06/02	SCA 1992/06/09	SCA 1992/06/25	melting 1992/06/02 to 1992/06/09	melting 1992/06/02 to 1992/06/25
Eastern position	-0.96	-0.95	-0.91	0.91	0.95
Average altitude per eastern position	0.97	0.96	0.91	-0.94	-0.93
Northern position	0.21	0.46	0.51	-0.83	-0.73

4.1.2 Altitude distribution

The SCA distributions with respect to altitude were found to be similar for all four occasions, irrespective of considered subdivisions of investigated area. *Figure 15* shows a typical example of the plots of SCA versus altitude. The SCA was increasing with altitude with two changes in the gradient coinciding with local maximas in SCA. From the altitude where snow first appears, SCA is strongly increasing up to ~900 m, where the first local maximum in SCA occurs. Above ~900 m there is a more gentle increase in SCA up to ~1250 m, where the next local maximum occurs. Above ~1250 m, the SCA is nearly constant. The maximas are coinciding with both gradient changes and also with altitudes that represent a great part of the investigated area. The altitudes at which the maximas occur are probably depending on topographic effects as explained in later sections. Furthermore, the maximas are caused by variations in SCA on gentle slopes (0-10°), while the steeper ones do not show same pattern (*Figure 16*). The difference in increase of SCA with altitude that occur at ~1250 m is not seen for steeper slopes.

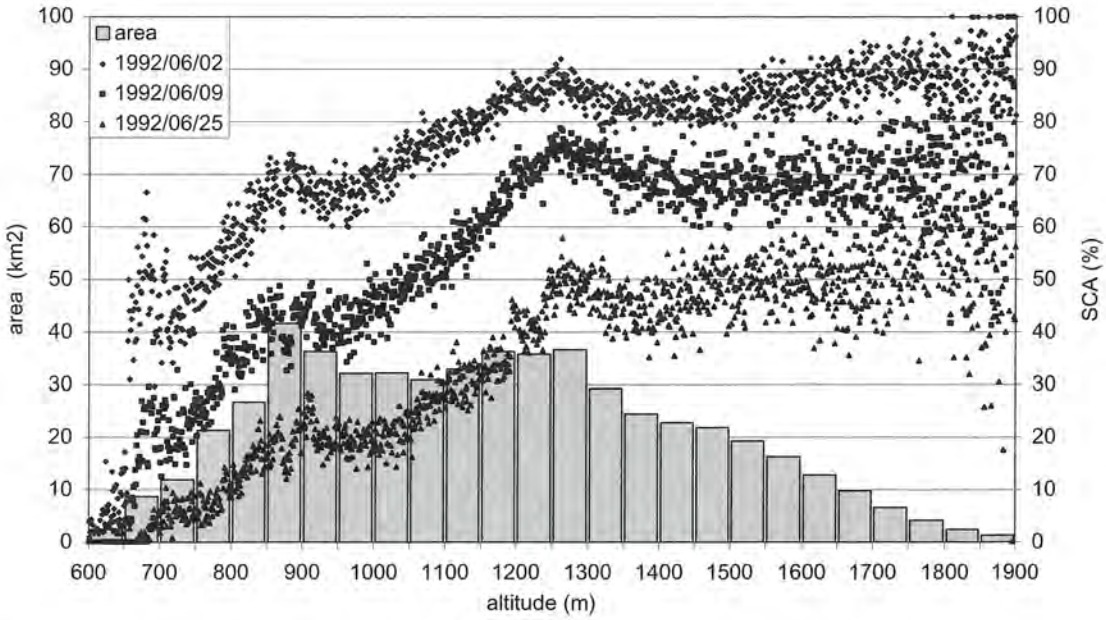

Figure 15 *The distribution of SCA with respect to altitude, in Laitaure.*

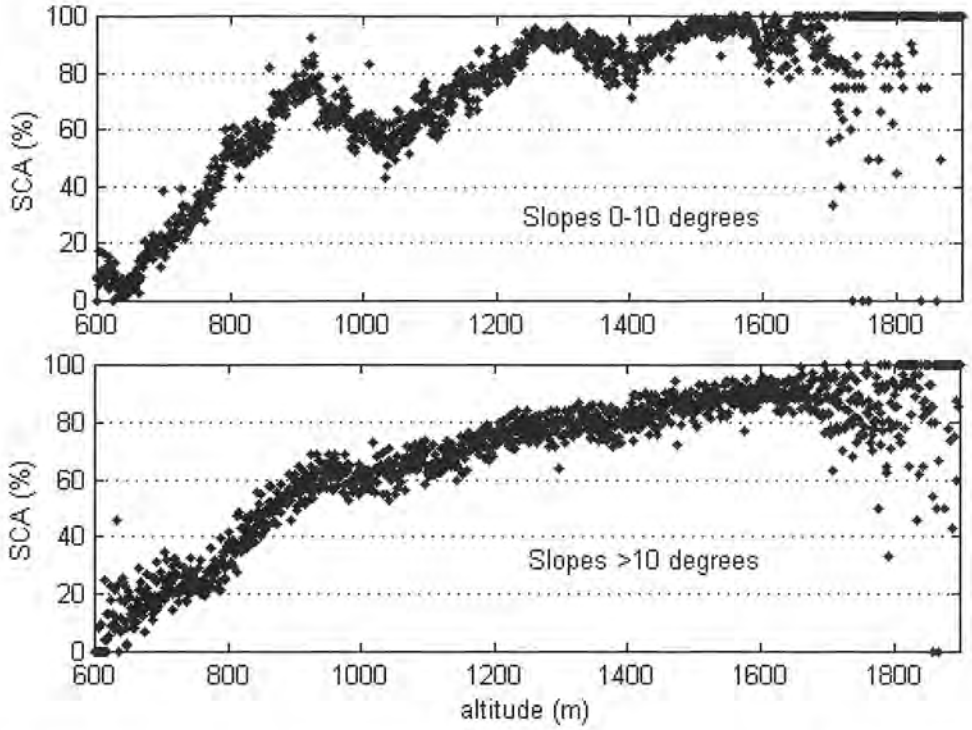

Figure 16 *Distribution of SCA 1992/06/09 with respect to altitude for gentle and steep slope clusters. Section A for all land covers except forest.*

4.1.3 Aspects distribution

SCA distributed on different aspects was found to have a quite similar pattern for different subdivisions of the investigated area and also for the different observations (1992/06/02, 1992/06/09, 1992/06/25 and 1996/06/04).

Figure 17 shows that, except for the flat areas which by definition do not slope in any direction, the eastern and southeastern aspects have the highest SCA, while the western and southwestern have the lowest. Moreover, the flat areas differ a lot in SCA depending on what subdivision of the investigated area that is considered. The observations of SCA from 1996/06/04 differ sligthly from that observed 1992. The differences between southwestern/western and southeastern/eastern aspects are not as big 1996 as 1992, but the difference between northern and southern aspects is greater.

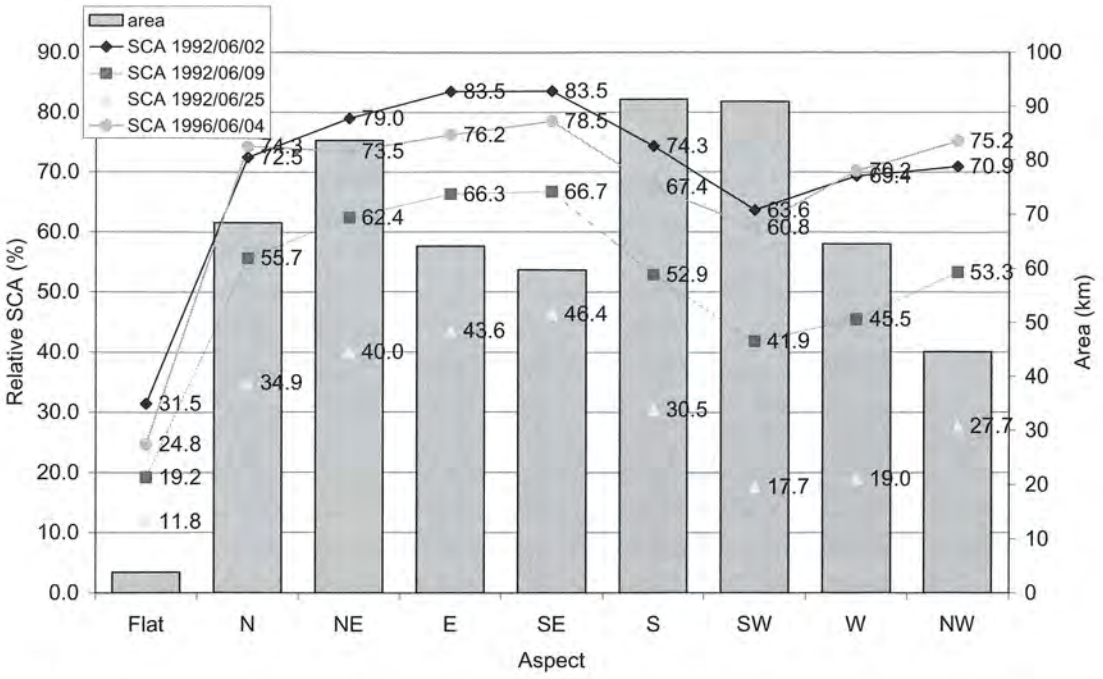

Figure 17 *Distribution of SCA with respect to aspects in Laitaure.*

As shown by *Table 8*, the distribution of SCA on different aspects is quite similar for different subdivisions of the investigated area. It should be noted that for altitude interval 901-1000 m in section A the extreme deviations are at W aspect and E aspect and not at SW and SE as for practically all other areas.

Table 8 *Deviation from average SCA (%) for different subdivisions of the total investigated area, aspects are sorted in ascending order for 1992 average in whole area*

Area	Date	SW	W	NW	S	N	NE	E	SE	average SCA (%)
Whole area	1992/06/02	-9.1	-6.9	-2.3	0.5	0.4	1.9	6.5	9.0	58.0
	1992/06/09	-10.1	-8.4	-0.5	-0.5	1.5	2.2	6.4	9.4	35.8
	1992/06/25	-8.6	-7.6	-1.2	-1.0	1.5	3.0	5.5	8.4	17.5
	average for 1992	-9.3	-7.6	-1.3	-0.3	1.1	2.4	6.1	8.9	
Section A	1992/06/02	-14.3	-6.0	4.3	-0.9	2.9	1.9	5.1	7.0	78.3
	1992/06/09	-16.0	-7.3	6.7	-1.5	2.5	0.6	5.5	9.5	62.2
	1992/06/25	-17.5	-12.2	1.7	-2.5	2.3	3.8	9.6	14.8	39.0
	average for 1992	-15.9	-8.5	4.3	-1.7	2.5	2.1	6.8	10.4	
Section A	1992/06/02	-10.9	-9.8	-5.6	2.4	3.7	4.4	8.5	7.3	79.0
901-1000 m	1992/06/09	-9.3	-12.3	-5.5	3.8	2.4	3.7	9.1	8.2	62.4
	1992/06/25	-12.4	-16.6	-10.5	-1.9	2.3	12.3	15.2	11.6	33.0
	average for 1992	-10.9	-12.9	-7.2	1.4	2.8	6.8	10.9	9.0	
Section A	1992/06/02	-17.2	-5.9	3.2	-2.2	1.4	5.0	8.1	7.6	86.4
1201-1300 m	1992/06/09	-20.8	-5.5	6.9	-5.5	1.4	2.1	10.0	11.3	75.4
	1992/06/25	-20.4	-14.6	-2.2	-5.9	3.5	3.2	18.0	18.5	54.2
	average for 1992	-19.5	-8.7	2.6	-4.5	2.1	3.4	12.0	12.4	
Laitaure	1992/06/02	-13.4	-5.1	-2.5	-1.9	-3.8	4.9	10.0	11.8	68.2
	1992/06/09	-15.4	-10.2	-2.9	-2.9	-1.8	7.8	12.1	13.3	52.4
	1992/06/25	-16.6	-14.8	-6.2	-1.9	0.6	9.4	13.7	16.0	34.3
	average for 1992	-15.1	-10.1	-3.9	-2.3	-1.7	7.4	11.9	13.7	
	1996/06/04	-11.2	-1.8	3.1	-4.6	2.3	1.4	4.2	6.5	

The correlations for SCA turned out to be higher for east-aspect than for north-aspect, see *Table 9*. The melting was as above calculated as the relative difference in SCA. The correlations for the observation from 1996 differ considerable from the ones from 1992.

Table 9 *Correlations between SCA and N-aspect/E-aspect respectively*

	1992/ 06/02	1992/ 06/09	1992/ 06/25	1996/ 06/04	melting 1992/06/02 to 1992/06/09	melting 1992/06/09 to 1992/06/25
N-aspect, section A	0.36	0.31	0.19		-0.25	-0.14
E-aspect, section A	0.66	0.60	0.82		-0.49	-0.92
N-aspect, Laitaure	0.00	0.16	0.12	0.45	-0.33	-0.03
E-aspect,Laitaure	0.91	0.92	0.94	0.58	-0.86	-0.94

The SCA was correlated with wind directions, and observations from 1992 were found to be highly correlated with directions measured at Pårtetjåkkå 1914-1916 and the geostrophic wind directions for the winter 1991/1992 (*Table 10*). SCA from 1996 had lower correlations with wind direction, maximum correlation was obtained for the directions measured at Pårtetjåkkå though. The high correlations between SCA from 1992 and wind directions are also evident from *Figure 18*, where an almost inverse relation between wind direction and SCA is seen.

Table 10 *Correlations between SCA and wind directions in Laitaure*

	Wind Pårtetjåkkå July 1914 - June 1916	Geostrophic wind Nov 1991 - May 1992	Geostrophic wind 1981-1990 & 1993-1998	Geostrophic wind Nov 1995 - May 1996	Geostrophic wind 1981-1994 & 1997-1998
SCA, Laitaure 1992/06/02	-0.95	-0.86	-0.75	-0.17	-0.79
SCA, Laitaure 1992/06/09	-0.92	-0.90	-0.86	-0.35	-0.88
SCA, Laitaure 1992/06/25	-0.90	-0.93	-0.89	-0.36	-0.91
SCA, Laitaure 1996/06/04	-0.74	-0.59	-0.63	-0.45	-0.63
Wind Pårtetjåkkå July 1914 – June 1916	1.00	0.88	0.78	0.21	0.81
Geostrophic wind Nov 1991 – May 1992	0.88	1.00	0.93	0.37	0.95
Geostrophic wind Nov 1995 – May 1996	0.21	0.37	0.64	1.00	0.58

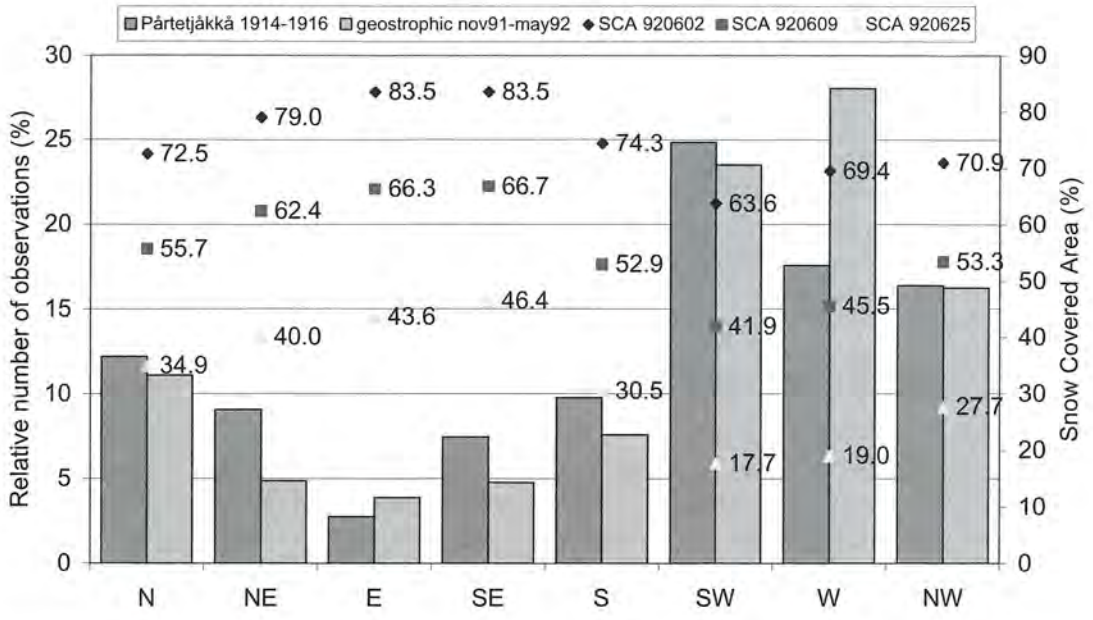

Figure 18 *Wind directions and SCA with respect to aspect in Laitaure.*

4.1.4 Slope distribution

Scatter plots of SCA versus slope show that SCA has a maximum for slopes ~23° (*Figure 19*). When investigating the whole area, this pattern is even more obvious, also for Laitaure. The SCA was on certain aspects found to have a somewhat different distribution over slope than on other aspects. For the gentler slopes ~<4°, the distribution is similar for different aspects but from 4 to ~20° there is an increasing difference in SCA on east and west aspects. For 1992/06/02 in Tjaktjajaure maximum SCA for clustered aspect NW, W and SW is obtained for slopes ~5° and for the NE, E and SE aspect ~20° (*Figure 20*).

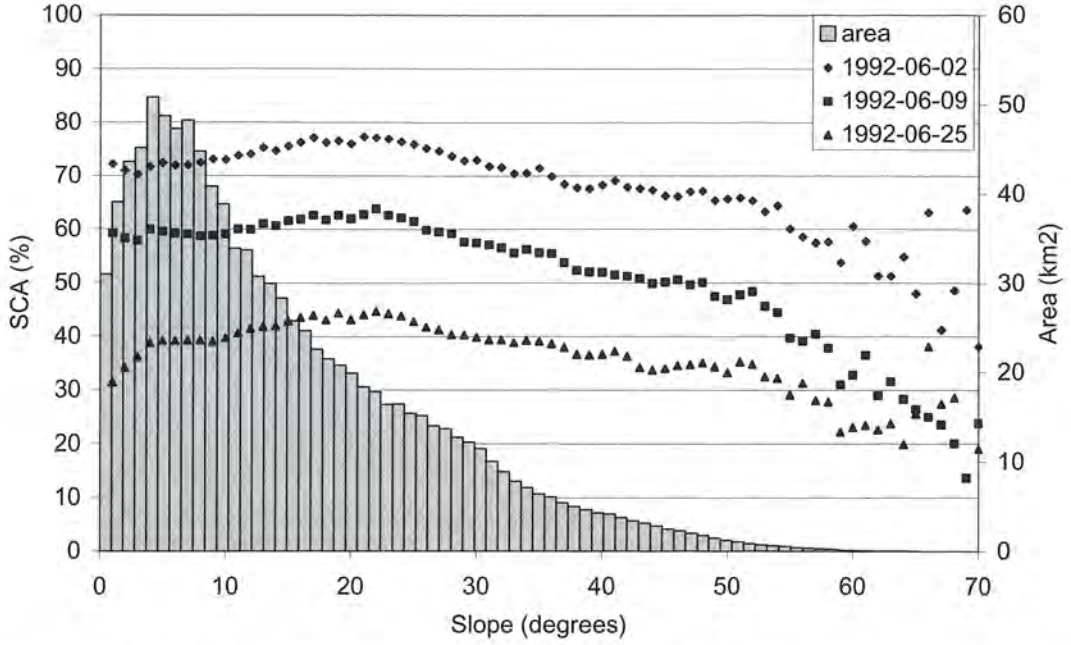

Figure 19 *Distribution of investigated area and SCA with respect to slope in Section A.*

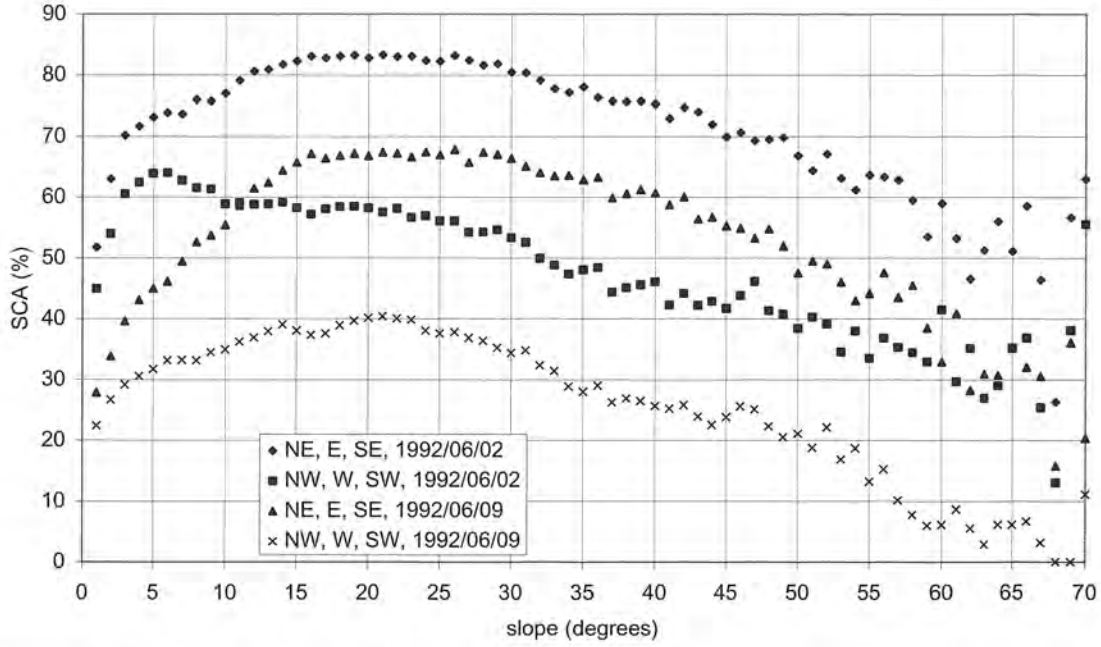

Figure 20 *Distribution of SCA on clustered aspects with respect to slope angle in Tjaktjajaure.*

Also, the melting (relative difference in SCA) was investigated with respect to slope. For section A, the melting increased with increased slope from 1992/06/02 to 1992/06/09 and decreased with increased slope from 1992/06/09 to 1992/06/25.

4.1.5 Land cover distribution

The SCA was, for the three most investigated land covers, highest for mountains (not forested), then wetlands and open ground (*Figure 21*). This order of SCA on the three land covers follows the distribution of them with altitude (*Figure 10*).

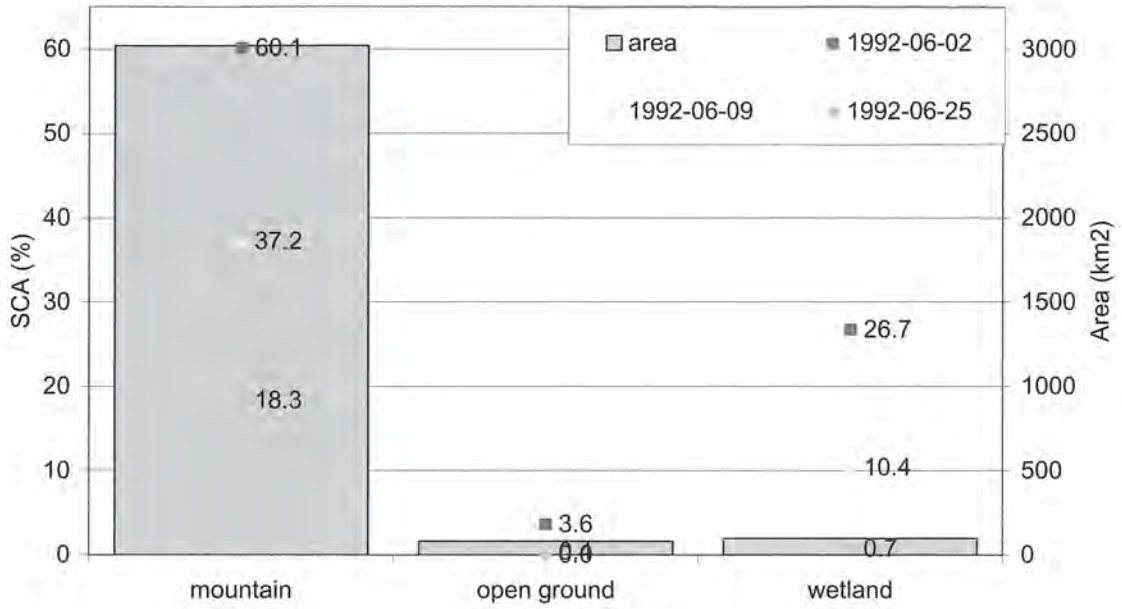

Figure 21 *Distribution of investigated area and SCA on different land covers. Whole investigated area.*

4.2 AN APPROACH FOR MODELLING SNOW DISTRIBUTION

Based on the empirical snow distribution results, the proposed distributed model can be specified:

1. The model is to be distributed in a grid-mesh.
2. An elevation correction is to be applied on precipitation and temperature.
3. All fallen snow above the timberline is to be distributed evenly on all altitudes above the timberline.
4. The accumulation correction for aspect must be calculated depending on the slope. Within interval 0° to ~23° the correction for each aspect should vary linearly from 1 to the aspect-specific number given in *Figure 22* (with lowest values on the aspect facing the wind). For slopes steeper than ~23°, the aspect correction is to be constant as in *Figure 22*.
5. Further, accumulation must be corrected for the steepest slopes by a factor decreasing from 1 at 23° to 0 at 90°.
6. The melt factor varies with aspect and have a maximum in southwest. The absolute numbers of the melt factor need to be chosen carefully but a start could be to use the variations in *Figure 23*.
7. In some regions it might be relevant to let the melt factor vary with slope as well. Hereby, the pattern in *Figure 1* should be strived for.

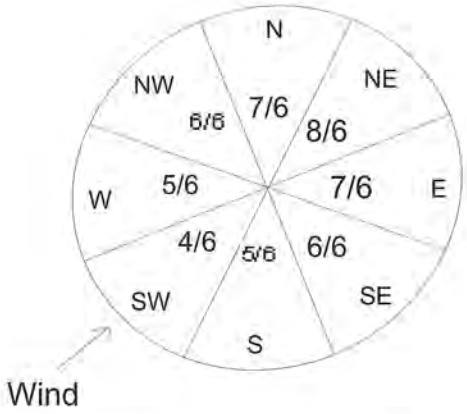

Figure 22 *A suggestion for accumulation correction when the dominating wind is from southwest.*

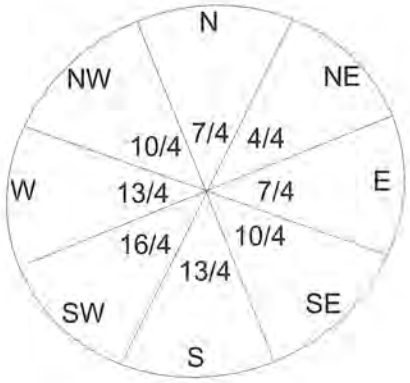

Figure 23 *Suggestion for melt factor varying with aspect. To be used with a timestep of one day. (Modified after Kirschbaum 1998.)*

The simplest way to model spatial snow distribution is to use a grid-mesh. Accumulation and ablation can thus be calculated specifically for each grid-cell. Also, precipitation and temperature can be different for different cells.

The accumulation of snow is due to precipitation (as extrapolated from meteorological stations with respect to altitude). The redistribution of snow by wind is to be included in the model. A simple way is to modify the precipitation by correction with respect to altitude, aspect and slope. A first attempt to modify accumulation with respect to aspect may be to distribute fallen snow as to obtain twice the amount on leeward slopes as compared to windward slopes, see *Figure 22* for illustration.

The melting of snow is to be calculated in the same way as by Kirschbaum (1998), i.e. according to the degree-day method in equation 7. Temperature to be used is the one extrapolated from meteorological stations with correction for altitude. Since the melting seen in the results in chapter 4.1 obviously differ on different aspects, a correction needs

to be done. To obtain different melt rates on different aspects the melt factor can be dependent on aspect, a first attempt may be to use melt factors as in *Figure 23*.

4.2.1 Model resolution

The variations in average N-aspect and E-aspect for grid cells of increasing size show that the difference between cells decreases. An example of this is shown in *Figure 24* for N-aspects. The difference is smoothened and decreased in the cell size interval 5000 to ~12000 m. In *Figure 25* same investigation is shown for E-aspect and the difference is relatively small for grid cells bigger than 8000 m.

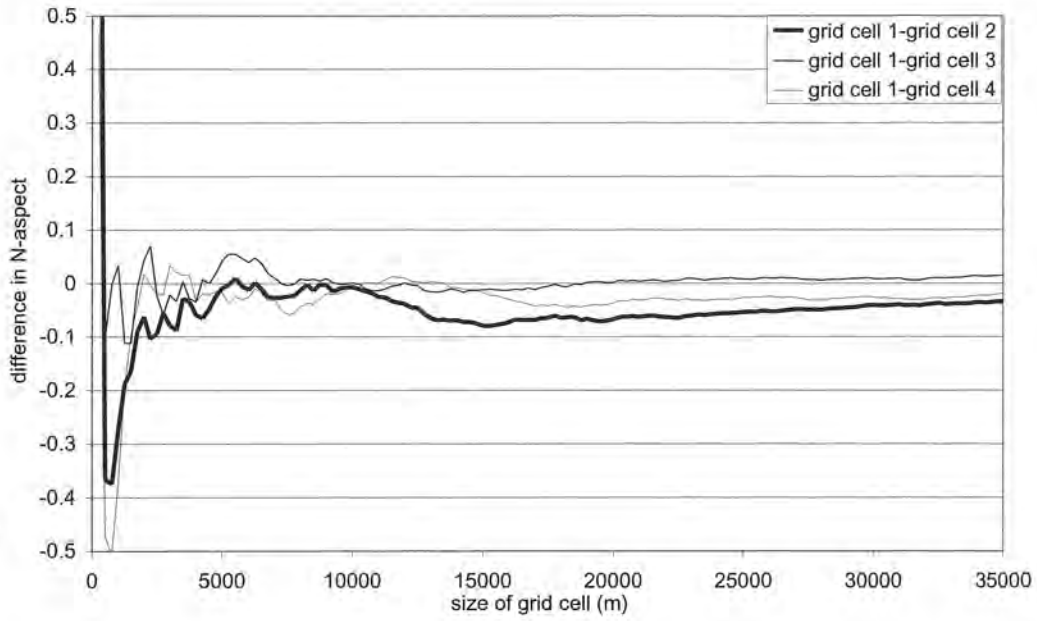

Figure 24 *Resolution control, difference in N-aspect between cells.*

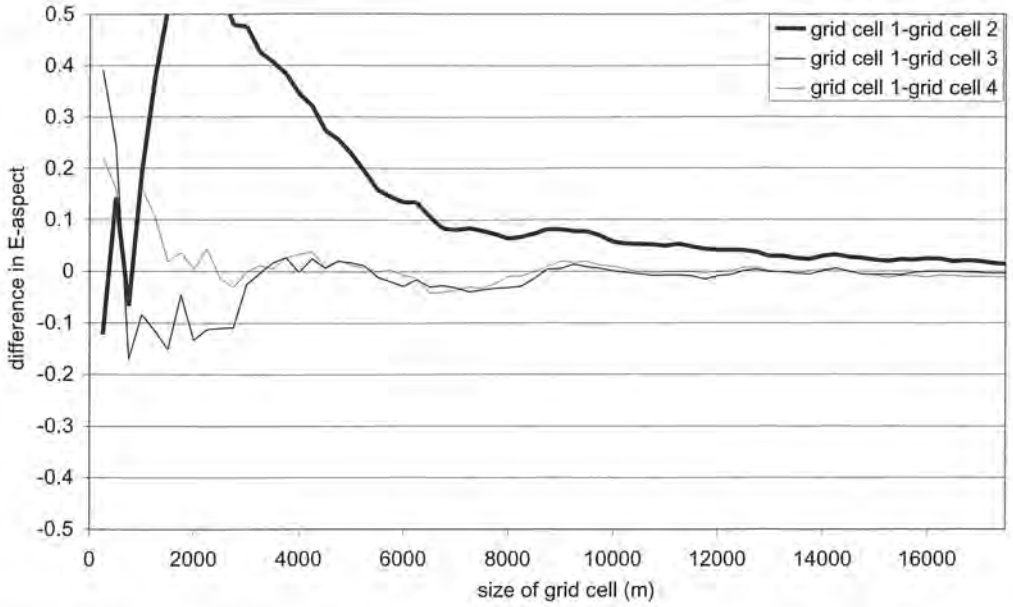

Figure 25 *Resolution control, difference in E-aspect between cells.*

To investigate the effect of resolution on model results, different assumptions about snow distribution with respect to slope and aspect were evaluated. These assumptions were further combined with assumptions about the distribution of temperature and precipitation with respect to elevation. If altitude information was to be considered, the precipitation (in the form of snow) was according to *Figure 26*. Otherwise it was assumed to be 400 mm. Corrections for accumulation were calculated by multiplying each grid-cell with a factor according to *Table 11*. Melting was calculated for ten days according to equation 7 with a threshold temperature of 0° C. If altitude was considered, the temperature was assumed to be as in *Figure 26*. Otherwise it was assumed to be 6°C. The melt factor was varied according to the approaches in *Table 11*.

Table 11 *Approaches for aspect-corrections used in resolution controls*

Approach 1	Flat	N	NE	E	SE	S	SW	W	NW
Melt factor (mm/°C day)	2.5	1.75	1	1.75	2.5	3.25	4	3.25	2.5
Accumulation correction	1	1.17	1.33	1.17	1	0.83	0.67	0.83	1
Approach 2	Flat	N	NE	E	SE	S	SW	W	NW
Melt factor (mm/°C day)	2.5	1	1.75	2.5	3.25	4	3.25	2.5	1.75
Accumulation correction	1	1	1.17	1.33	1.17	1	0.83	0.67	0.83
Approach 3	Flat	N	NE	E	SE	S	SW	W	NW
Melt factor (mm/°C day)	2.5	1.75	1	1.75	2.5	3.25	4	3.25	2.5
Accumulation correction	1	1	1	1	1	1	1	1	1
Approach 4	Flat	N	NE	E	SE	S	SW	W	NW
Melt factor (mm/°C day)	2.5	2.5	2.5	2.5	2.5	2.5	2.5	2.5	2.5
Accumulation correction	1	1.17	1.33	1.17	1	0.83	0.67	0.83	1

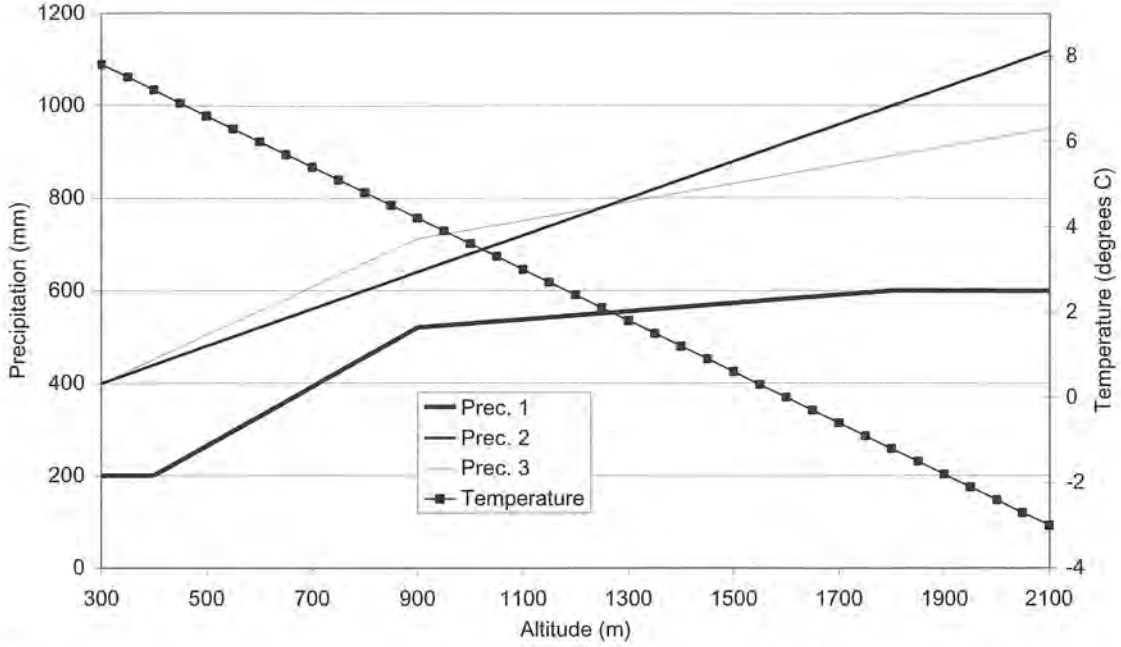

Figure 26 *Assumed temperature and precipitation used for resolution control.*

The results considering snow amounts corrected for only aspect show a reduction in differences between cells at the cell size ~10000 m and larger. All tests for the four approaches were very similar to the examples shown by *Figure 27* and *Figure 28*. The critical cell size for no clear difference between cells due to aspects are not completely clear but it seems to be approximately 10000 m $^{+}$/- 5000 m.

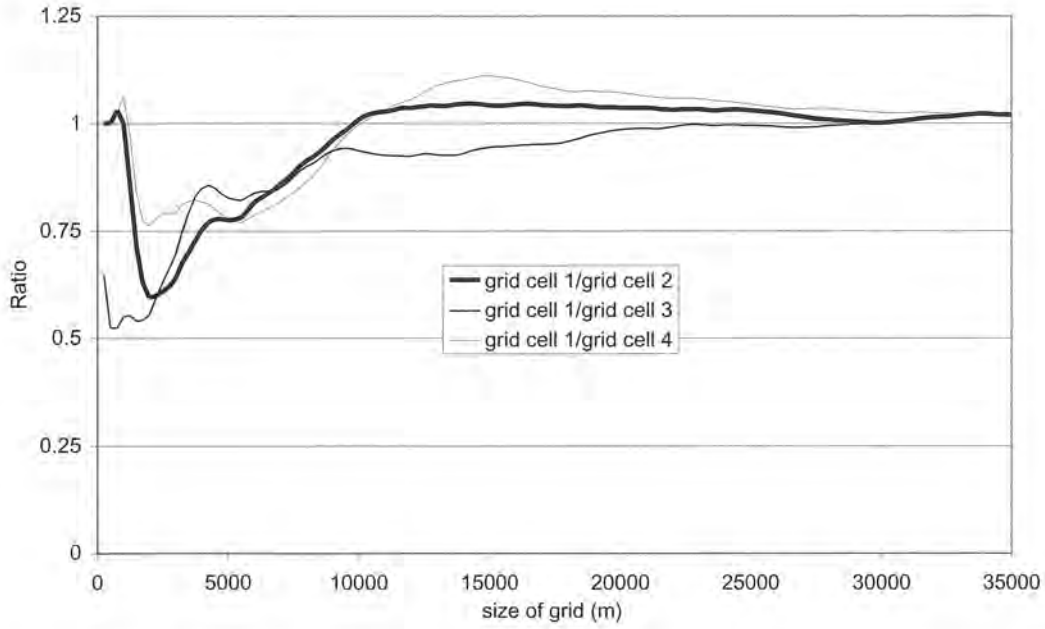

Figure 27 *Resolution control, ratios between snow amounts in different grid cells corrected for aspects according to approach 4.*

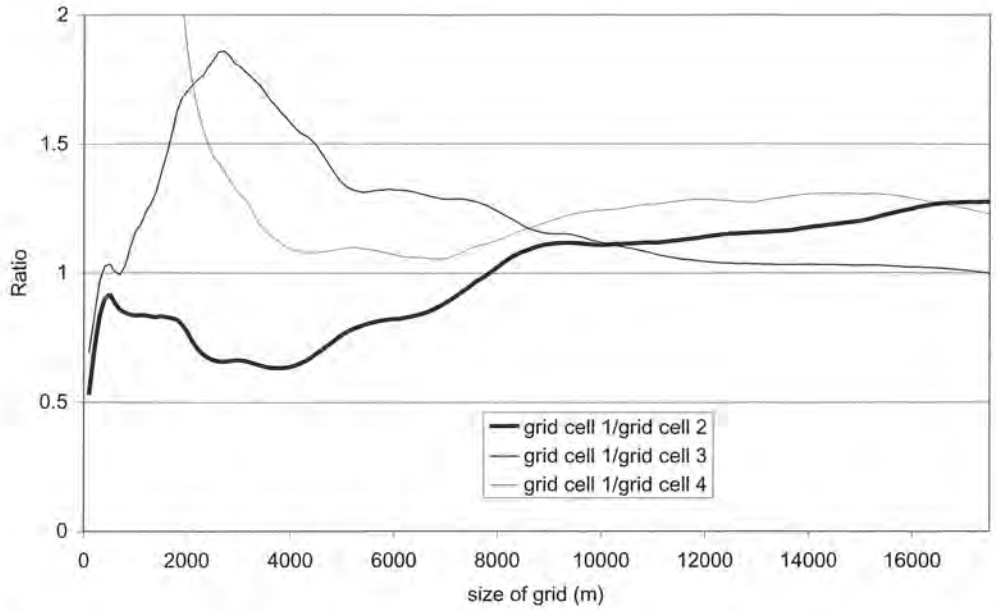

Figure 28 *Resolution control, ratios between snow amounts in different grid cells corrected for aspects according to approach 1.*

When including the correction for altitude in calculations of snow amounts, the altitude was found to be the most important factor. An example of ratios between cells when considering both aspect and altitude is shown in *Figure 29*. No critical cell size what concerns snow amounts corrected for altitude is found on this scale.

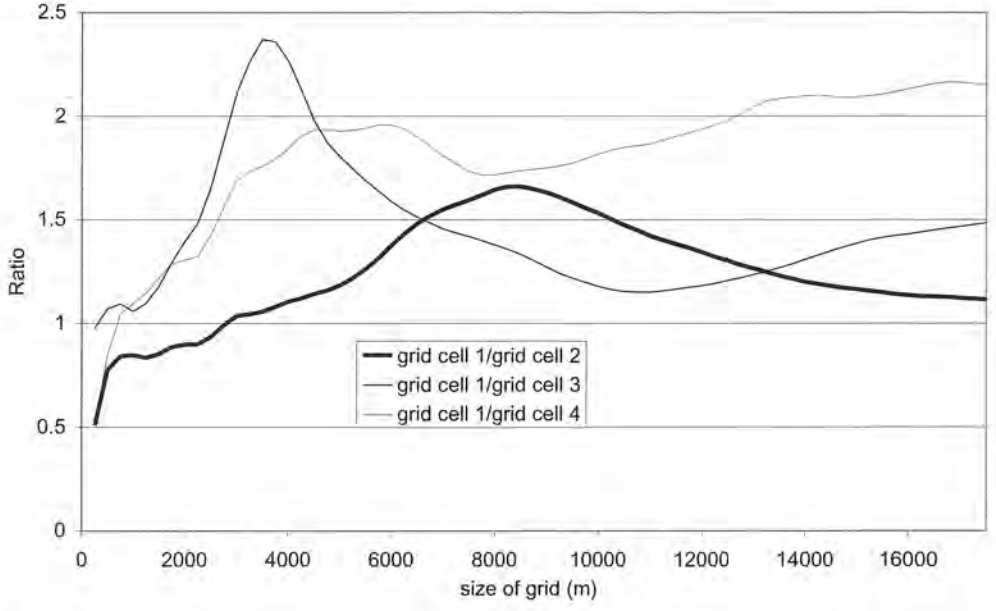

Figure 29 *Resolution control, ratios between snow amounts in different grid cells. Snow amounts corrected for aspects according to first approach and precipitation vary with altitude according to assumption 1.*

5 DISCUSSION

5.1 TOPOGRAPHIC FEATURES IN THE INVESTIGATED AREA

The altitude varies with geographical position and seems to be the determining factor for the location of forested areas. Altitude decreases with eastern co-ordinate and this may explain why the precipitation is lower in the eastern areas. The relative area of NW and SE aspects is increasing with height, since the slopes in these directions are more gentle at higher altitudes than other slope directions. However, east aspects have less relative area at higher altitudes, which can be explained by "skollorna" (see for instance Lindström et al. 1991) that occur in the Scandinavian mountains and which cause steep slopes to face east.

Since the resemblance between Pårtetjåkkå-wind and geostrophic wind is high, it seems likely that the present winds at Pårtetjåkkå are similar to those measured in the early 20th century. Furthermore, the coinciding pattern between geostrophic wind and wind at Pårtetjåkkå implies that the wind at Pårtetjåkkå can be assumed to be valid for most part of the investigated area. Accordingly, the wind directions at Pårtetjåkkå from 1914-1916 give a good estimate of normal wind conditions in the area, even for the periods when observations of SCA exist for this study. Since glaciers are situated in places with high accumulation they are also a sort of index for what aspects receive extra snow from redistribution with wind. The glaciers are mostly situated on north-eastern and eastern aspects, which indicates that the wind is (or have been) dominated by south-western and western winds.

5.2 SNOW DISTRIBUTION

Geographical position

The distribution of snow depends strongly on the eastern position. This is mainly explained by the fact that the altitude is decreasing and partly due to the precipitation variation with eastern position (Bergström & Brandt 1984). The altitude decreases with eastern co-ordinate. Therefore, temperature is higher and precipitation lower in the eastern regions and the SCA becomes lower. Hence, the lower SCA is a result of lower altitude and not primarily longitude. The high correlation between the relative difference in SCA (melting) and eastern co-ordinate is probably also an effect of mentioned altitude variations.

The variation of melting with northern co-ordinate is probably due to aspects since the melting is more pronounced on the south-facing slopes than on the north-facing slopes. (The northern regions have larger areas with north-facing slopes and the southern regions have larger areas with south-facing slopes.)

Aspect

The variations in SCA with north-aspect are probably partly explained by the varying conditions for solar radiation. According to theory, greater differences between north and south facing slopes could be expected. However, the region has many days with overcast and the direct solar radiation may thus not be as important as suggested by *Figure 1*. Also, the observations of SCA are from June, when the sun is above the horizon for a long part of the day and does not vary much in solar elevation. This means that

during June the differences in solar radiation on aspects at this latitude are smaller than shown by *Figure 1*.

The southwest-facing slopes have lower SCA than the south-facing slopes. This can be explained by the combined effect of temperature and radiation, which Hock (1999) successfully has modelled. Physically, this may be explained assuming a melt period with melting during daytime and cooling of the snow pack during night. Every morning the snow pack needs to get reheated to 0° C before melting can start. Thus, southwest facing slopes are exposed to maximum solar radiation at the time of day when temperature is at maximum. The southeast-facing slopes, on the other hand, obtain maximum solar radiation before midday, when the temperature may not even have raised to 0° C. This explanation is given by Baumgartner & Apfl (1997) and is supported by simulations done by Rango & Martinec (1995).

Further, the observed snow distribution is also most certainly an effect of wind redistribution of snow. The SCA is higher on the northeast/east/southeast aspects than on the northwest/west/southwest aspects which is a clear indication that the wind has transported snow from west to east. Furthermore, the distribution of the glaciers also indicates this transport of snow by wind. This is also supported by the high correlation between wind directions and SCA. *Figure 4* shows that the south-westerly winds are most common and thus the highest SCA should be expected on the north-eastern aspects (as for the glaciers). But, since the eastern and north-eastern aspects are less common at higher altitudes they may have lower SCA than they would have if they were equally distributed on all altitudes (since SCA is higher for higher altitudes). Thereby, if the north-eastern aspects were equally distributed on all altitudes, the difference in SCA between south-west and north-east aspects would probably increase. Accordingly, the reason for SCA being lower on north-east aspects than east and south-east aspects might be a result of the relatively low area of north-east aspects at higher altitudes.

Moreover, the higher wind speeds at slopes facing the wind (southeastern aspects) cause higher energy exchanges and thus more efficient melting when it occurs.

The results are to a high extent coinciding with those obtained by Ehrler et al. (1997) in Switzerland. These distributions of snow on different aspects are therein said to be a result of wind patterns and solar raditation.

Slopes

The observed snowcover on different slope angles is strongly affected by the fact that slope angles have different distributions over altitude. Within the slope interval 0 to ~20° SCA is increasing with increased slope angle, which corresponds to the altitudal distribution of slopes in this interval. The flat and most gentle slopes are more common at lower altitudes while the relative areas of >23° slopes are increasing with altitude.

The situation is different for slopes steeper than ~23°. Even though the steepest slopes are more common at higher altitudes, the SCA is decreasing with increased slope. Here, other factors than merely altitude affect the distribution of SCA. The steeper slopes are more affected by wind, which causes snow to be transported away from them. Another reason for low SCA on the steepest slopes is gravity. According to Seligman (1936), avalanches occur on slopes steeper than 22°. Thus, the steep slopes may have lost snow to the gentler slopes.

Maximum SCA is obtained for ~23° slopes which is a similar result to those achieved by Rawls & Jackson (1979), who observed maximum accumulation for 18.5° slopes. A local minimum at ~30-45° may have been expected due to the solar radiation but is not seen in the slope-distribution of SCA.

The slope-distribution of SCA is similar for different subdivisions of the investigated area. However, some differences are observed in the increase of SCA in the interval 0 to ~20°. Section A has less flat and gently sloping areas at lower altitudes than what is present in the area as a whole. Thereby, the gradient in SCA versus slope is smaller in section A.

Figure 20 shows the difference between aspects on gentle slopes, down to 3°. From 3° to ~20° the difference increases while it is approximately constant for steeper slopes. This shows to what extent there is a difference between the aspects. Slopes do not have to be steeper than 3° to be affected by aspect-related processes, and the absolute differences in SCA attributed to those processes are greatest for slopes of 20° or steeper.

Altitude

SCA is increasing considerably with altitude. The explanations to this are the precipitation and temperature conditions that vary with altitude. The change in SCA increase with altitude at ~900 m is probably caused by the timberline which occur at approximately this altitude. This is suggested by Bergström & Brandt (1984), who found that SWE increases with altitude up to the timberline and is approximately constant above due to the great redistribution of snow by wind. Even though the forest is excluded from most investigations in this study it may also affect the results. Areas at altitudes where a forest is present may be affected by the forest even if it is not in a close vicinity. The forest causes great friction against air masses that passes by and thus affects wind patterns over wider ranges than within the forested area itself. Furthermore, the distribution of unforested mountain with altitude (see *Figure 10*) shows a slight change in the increase of cumulative area at the altitude ~900 m. This means that the areas of mountain at altitudes higher than ~900 m are smaller than below. Thereby, the air mass above ~900 m is less affected by friction from the ground and consequently has higher wind velocities. This is a second reason for higher redistribution of snow at altitudes above ~900 m and a reduction in the gradient SCA versus altitude.

Since the data for this study show an increase in SCA even above the timberline, at least one factor affecting the snow is different in this study compared to the study presented by Bergström & Brandt (1984). The results presented by Bergström & Brandt (1984) were from measurements earlier in the spring. It can thus be assumed that those were not as affected by melting as the data in this study. Hence, it is likely that the observed increase of SCA with altitude, above ~900 m, is caused by the altitude-dependence of temperature.

The local maximum that occur at ~900 m is caused by higher SCA on the gentle slopes and flat areas. These areas are more usual at this altitude than that altitudes direct above and below. The altitude ~900m has several areas surrounded by high peaks, which implies that the peaks shield these areas from wind. In addition, the relative areas of NW, W and SW aspects are smaller than directly above and below ~900 m, and the opposite is valid for SE aspects. This is also an indication that the number of wind shielded

places at ~900 m is relatively high. So, the increased local maximum of SCA at ~900 m is probably a pure topographic effect, where the terrain creates several spots at ~900 m shielded from wind. Thus, snow is redistributed from the higher, wind-exposed peaks down to the gently sloping or flat wind-shielded areas at ~900 m.

There is also an indication of a second change in the gradient of SCA versus altitude (at ~1250 m). The change in gradient also coincides with a local maximum which is caused by high SCA on the flat and gently sloping areas. Besides from large areas of gentle slopes (see *Figure 8*), this specific altitude has relative large areas of SE aspects (see *Figure 6*). The reasons to this local maximum seem to be the same as for the local maximum at ~900 m, though it is not as large as the lower one since the topographic anomalies are not as big and many. The reason to the slight change in the gradient at ~1250 m is not as obvious as for the one at ~900 m. The gradient change might be a result of the terrain above ~1250 m having steeper slopes and being dominated by peaks situated at relatively far distance from each other, i.e. the areas above ~1250 m are more exposed to wind. This is further indicated by the second slight change in cumulative area of unforested mountain with altitude. So, the second change in the gradient SCA versus altitude is caused by the same factors as the first change, even though the second is not as great.

Land cover
The observed differences in SCA on land cover seem to be dependent on the altitude distribution of those land covers. If altitude, aspect and slope are considered, there is probably not any significant difference in SCA on the land covers; mountain (unforested), open ground and wetland.

5.3 PROPOSED MODELLING APPROACH

A model in a grid-mesh has several advantages. The SMHI-project aims to create snow maps from modelling combined with satellite data. The satellite images are given as grid-meshes and are therefore easily combined with a model in the form of a grid-mesh. Also, since the digital elevation maps are in grid-meshes this form makes the connection between the model and elevation data easier. A further advantage is that the grid-meshes are easily presented graphically with simple presentations.

With the suggested modelling approach only temperature and precipitation are needed when running the model which makes the interpretation easy. To set up the model, the required information is a digital elevation map, statistics of wind directions and information about cloudiness. All information is easily available. Elevation maps exist with high resolution and wind directions can be obtained from synoptic data.

The redistribution of snow by wind is included by the multiplication of precipitation with aspect-specific factors. These aspect-specific factors are suggested under the assumption of twice the amount of snow on leeward slopes compared to the windward slopes. If there exist data on snow distributions for the area to be modelled, these data can be used to reassess the aspect-specific factors. The redistribution of all fallen snow above the timberline is another effect of the redistribution of snow by wind. To separate the most gentle slopes from the steeper, the differences between the aspect-specific corrections are increasing in the slope interval 0° to 23°. Slopes steeper than 23° are multi-

plied with an extra factor (that is varying from 1 at 23° to 0 at 90°), which is to include the loss of snow from these slopes due to gravity and wind.

The use of a degree-day method does not demand one or more extra input variables but allows the melt factor (CFMAX) to vary depending on a number of different spatially varying factors. Since the melting varies with different solar radiation conditions, the melt factor is modified with respect to aspect. The most straightforward correction would have been to use a melt factor that gives maximum melt on south aspects and minimum on north aspects. Due to the results of chapter 4.1 and the modelling results by Hock (1999), it seems as the maximum is obtained for southwest aspects instead of south. Using a melt factor with a maximum in south, this pattern will not be obtained when using a timestep of one day or more. Therefore, the maximum melt factor is suggested to occur on southwest-facing slopes. If a shorter timestep is to be used, e.g. 1 hour, then the melt factor probably will not vary that much with respect to aspect. The amount of variation in melt due to solar radiation is difficult to estimate and further investigations are needed before a reasonable distribution can be recommended. Obviously, this is depending on the local weather situations on different places. If it is cloudy, the difference in melting on aspects should be less than for areas with mostly clear sky. The absolute values of the melt factor will probably be an issue for calibration.

According to theory, the slope correction for melting should be of the distribution shown in *Figure 1*. However, the results in chapter 4.1 do not coincide with the theory. As mentioned earlier, this may be a result of the relatively high cloudiness in the investigated area. Depending on the area to be modelled, it might be of relevance to include a slope-correction for the melt factor. If so, the melt factor must decrease with increased slope for north aspects and have a maximum around 30-45° for south aspects.

Model resolution

The resolution controls shows that the pattern of varying snow amounts on different aspects are seen on scales up to at least 5000 m. Therefore, the difference due to aspects can be caught even in models with low resolution. Hence, models with low resolution do also have an opportunity to get better performance by including information about aspects. There does not seem to be a critical cell size where the difference between cells due to their average altitude is not detectable.

6 CONCLUSIONS

The snow covered area (SCA) in a mountainous area in Sweden was found to be dependent on altitude. SCA increases linearly with altitude up to the timberline. Above the timberline, SCA is nearly constant. Deviations from this pattern are explained by topographic factors, such as aspect and slope angle, that affect the accumulation and ablation processes. The variation of SCA with respect to aspect is governed by redistribution of snow by wind and melting by the combined effect of solar radiation and temperature. SCA varies with slope angle due to gravity and wind. Also, the difference between aspects increases for slope angles from 0° to 20° and is then constant for steeper slopes. Accordingly, redistribution of snow by wind is the most important process that is dependent on slope aspect and slope angle. As a consequence, the snow distribution in an area can to a large extent be explained by means of a digital elevation map and wind statistics.

Snow maps can be made by combining satellite images and a distributed snow model. A grid-mesh is a suitable type for the distributed model and the snowpack can thus be modelled separately in each grid-cell. (Each grid-cell is thereby a single model of the snowpack.) The degree-day method is a simple approach for a model that is easy to interpret for each grid-cell. Corrections for accumulation and ablation can be done considering the topographic characteristics for each cell. Accumulation, as observed from meteorological stations must be corrected for altitude, slope aspect and slope angle of the cell. Ablation in the form of melting should be calculated with a degree-day factor that depends on slope aspect and possibly even slope angle. This approach of modelling snow within each cell is feasible for resolutions up to at least 5000 metre. For lower resolutions the effect of aspects may not completely be identified.

7 ACKNOWLEDGEMENTS

The Landsat TM images were originally processed for the HydAlp project by Owen Turpin at the Sheffield Centre for Earth Observation Sciences, University of Sheffield. HydAlp (Hydrology of Alpine and High Latitude Basins) was a CEO Shared Cost Action Project of the European Union DGXII Specific Programme for Climate and Environment (ENV-CT96-0364).

This Master Thesis Work had not been possible without my supervisor Barbro Johansson at SMHI, whom I would like to thank for excellent guidance, quick responses and professional help. Also, I would like to thank the whole staff at the Division for Research and Development at SMHI. Whatever my question, there has always been someone taking the time to help me out. In particular Anders Gyllander, Weine Josefsson, Haldo Vedin and Håkan Hultberg, all at SMHI, have been very helpful.

Finally, I would like to thank Lars-Christer Lundin at the Division for Hydrology, Uppsala University, for being the examiner of this Thesis Work.

8 REFERENCES

Barry, R.G., 1981. *Mountain weather and climate*, Methuen & Co., New York.

Baumgartner, M.F. & Apfl, G.M., 1997. "Remote sensing, geographic information systems and snowmelt runoff models – an integrated approach." Remote Sensing and Geographic Information Systems for Design and Operation of Water Resources Systems (Proceedings of Rabat Symposium S3, April 1997) IAHS Publ. No. 242, 73-82.

Bergström, S. & Brandt, M., 1984. "Snömätningar med flygburen gammaspektrometer i Kultsjöns avrinningsområde." SMHI HO-Rapport, Nr. 21, 1984. (In Swedish).

Blöschl, G., Gutknecht, D. & Kirnbauer, R., 1991a. "Distributed Snowmelt Simulations in an Alpine Catchment 2. Parameter Study and Model Predictions." Water Resources Research, Vol. 27, No. 12, 3181-3188.

Blöschl, G., Kirnbauer, R. & Gutknecht, D., 1991b. "Distributed Snowmelt Simulations in an Alpine Catchment 1. Model Evaluation on the Basis of Snow Cover Patterns." Water Resources Research, Vol 27, No 12, 3171-3179.

Cline, D.W., Bales, R.C. & Dozier, J., 1998. "Estimating the spatial distribution of snow in mountain basins using remote sensing and energy balance modelling." Water Resources Research, Vol. 34, No. 5, 1275-1285.

Dozier, J., 1980. "A Clear-Sky Spectral Solar Radiation Model for Snow-Covered Mountainous Terrain." Water Resources Research, Vol. 16, No. 4, 709-718.

Dubayah, R., 1992. "Estimating Net Solar Radiation Using Landsat Thematic Mapper and Digital Elevation Data." Water Resources Research, Vol. 28, No. 9, 2469-2484.

Dubayah, R. & Rich, P.M., 1995. "Topographic solar radiation model for GIS." International Journal of Geographical Information Systems, Vol. 9, No. 4, 405-419.

Elder, K., Dozier, J., Michaelsen, J., 1991. "Snow Accumulation and Distribution in an Alpine Watershed." Water Resources Research, Vol. 27, No. 7, 1541-1552.

Ehrler, C; Seidel, K; Martinec, J., 1997. "Advanced analysis of snow cover based on satellite remote sensing for the assessment of water resources." In:Remote Sensing and Geographic Information Systems for Design and Operation of Water Resources Systems. IAHS Publication no. 242, pp. 93-101.

Föhn, P.M.B. & Meister, R., 1983. "Distribution of snow drifts on ridge slopes: Measurements and theoretical approximations." Annals of Glaciology, Vol. 4, 52-57.

Garnier, B.J. & Ohmura A., 1968. "A method of Calculating the Direct Shortwave Radiation Income of Slopes." Journal of Applied Meteorology, Vol. 7, 796-800.

Hamberg, A. & Jönsson, A, 1933. *Meteorologische Beobachtungen auf dem Pårtetjåkko (H = 1834 m ü. d. M, φ = 67°9'22,6'' N, λ = 17°37'57'' E v. Greenwich) während des Beobachtungsjahres 1. Juli 1914 bis 30. Juni 1915.*, C.E. Fritzes Bokförlags-Aktiebolag, Stockolm. (In German).

Hock, R., 1999. "A distributed temperature-index ice and snowmelt model including potential direct solar radiation." Journal of Glaciology, Vol. 45, No. 149, 101-111.

Jaedicke, C., Thiis, T.K., Sandvik, A.D. & Gjessing, Y., 2000. "Drifting snow in complex terrain; comparison of measured snow distribution and simulated wind field." Proceedings of the fourth international conference on Snow engineering; recent advances and developments., Rotterdam, Netherlands, 65-73.

Josefsson, W., 1985. "Solstrålning mot lutande ytor i Stockholm." Byggforskningsrådet, R128:1985. (In Swedish).

Kirschbaum, R., 1998. "Development of a gridded degree-day snow accumulation/ablation model with spatio-temporally varying melting factor." Norwegian Water Resources and Energy Directorate, Report No. 1.

Kuittinen, R., 1989. "Determination of snow water equivalents by using NOAA-satellite images, gamma ray spectrometry and field measurements." Remote Sensing and Large-Scale Global Processes (Proceedings of the IAHS Third Int. Assembly, Baltimore, MD, May 1989). IAHS Publ. No. 186, 151-159.

Klein, A.G., Hall, D.K. & Riggs, G.A., 1998. "Improving snow cover mapping in forests through the use of a canopy reflectance model." Hydrological Processes, Vol. 12, No. 10-11, 1723-1744.

Köhler, H., 1939. *Meteorologische Beobachtungen auf dem Pårtetjåkko (H = 1834 m Seehöhe, φ = 67°9'22,6'' N, λ = 17°37'57'' E v. Greenwich) während des Beobachtungsjahres 1. Juli 1915 bis 30. Juni 1916.*, Kungliga Vetenskapsakademien, Stockolm. (In German).

Leavesley, G.H., 1989. "Problems of snowmelt runoff modelling for a variety of physiographic and climatic conditions." Hydrological Sciences, Vol. 34, No. 6, 617-634.

Liljequist, G.H., 1962, *Meteorologi.* Generalstabens Litografiska Anstalt, Stockholm. (In Swedish).

Lindström, M., Lundquist, J. & Lundquist, T., 1991. *Sveriges Geologi från Urtid till Nutid.* Studentlitteratur, Lund. (In Swedish).

Lindström, G., Gardelin, M., Johansson, B., Persson, M. & Bergström, S., 1996. "HBV-96 – En areellt fördelad modell för vattenkrafthydrologin." SMHI RH, Nr. 12, april 1996. (In Swedish).

Liston, G.E. & Sturm, M., 1998. "A snow-transport model for complex terrain." Journal of Glaciology, Vol. 44, No. 148, 498-516.

Lodén, K., Liljequist, G.H. & Mathiesen, O., 1971. *Fysik – Astronomi och Geofysik.* Almqvist & Wiksell Boktryckeri AB, Uppsala. (In Swedish).

Male, D.H., 1980. "The seasonal snowcover." in *Dynamics of snow and ice masses.* edited by Colbeck, Samuel C., Academic Press Inc., New Hampshire, USA.

Male, D.H. & Granger, R.J., 1981. "Snow surface energy exchange." Water Resources Research, Vol. 17, No. 3, 609-627.

Malmström, B. & Wellving, A., 1995 *Introduktion till GIS.* Trycksam, Gävle. (In Swedish).

Ohta, T., 1994. "A distributed snowmelt prediction model in mountain areas based on an energy balance method." Annals of Glaciology, 19, 1994, 107-113.

Palmén, E. & Newton, C.W., 1969. *Atmospheric Circulation Systems – Their Structure and Physical Interpretation.* Academic Press Inc., New York.

Rango, A., 1993. "II. Snow Hydrology Processes and Remote Sensing" Hydrological Processes, Vol. 7, 121-138.

Rango, A. & Martinec, J., 1995. "Revisiting the degree-day method for snowmelt computations." Water Resources Bulletin, Vol. 31, No. 4, 657-669.

Rango, A. & Martinec, J., 1997. "Water storage in mountain basins from satellite snow cover monitoring." Remote Sensing and Geographic Information Systems for Design and Operation of Water Resources Systems (Proceedings of Rabat Symposium S3, April 1997). IAHS Publ. No. 242, 83-91.

Rawls, W.J. & Jackson, T.J., 1979. "Pattern Recognition Analysis of Snowdrifts." Nordic Hydrology, Vol. 10, No. 4, 251-260.

Rott, H., Nagler, T., Glendinning, G., Wright, G., Miller, D., Gauld, J., Caves, R., Ferguson, R., Quegan, S., Turpin, O., Clark, C., Johansson, B., Gyllander, A., Baumgartner, M., Kleindienst, H., Voigt, S., Pirker, O., 2000. "HydAlp. Hydrology of Alpine and High Latitude Basins. Final Report. (Contract ENV4-CT96-0364 for the European Union, DG XII)." Institut für Meteorologie and Geophysik, Universität Innsbruck, Mitteilung No. 4.

Sand, K. & Bruland, O., 1998. "Application of Georadar for Snow Cover Surveying." Nordic Hydrology, Vol. 29, No. 4/5, 361-370.

Seligman, G., 1936. *Snow structures and ski fields.* Macmillan & Co., London.

SMHI ger ut sex rapportserier. Tre av dessa, R-serierna är avsedda för internationell publik och skrivs därför oftast på engelska. I de övriga serierna används det svenska språket.

Seriernas namn	**Publiceras sedan**
RMK (Rapport Meteorologi och Klimatologi)	1974
RH (Rapport Hydrologi)	1990
RO (Rapport Oceanografi)	1986
METEOROLOGI	1985
HYDROLOGI	1985
OCEANOGRAFI	1985

I serien HYDROLOGI har tidigare utgivits:

1 Bengt Carlsson (1985)
Hydrokemiska data från de svenska fältforskningsområdena.

2 Martin Häggström och Magnus Persson (1986)
Utvärdering av 1985 års vårflödesprognoser.

3 Sten Bergström, Ulf Ehlin, SMHI, och Per-Eric Ohlsson, VASO (1986)
Riktlinjer och praxis vid dimensionering av utskov och dammar i USA. Rapport från en studieresa i oktober 1985.

4 Barbro Johansson, Erland Bergstrand och Torbjörn Jutman (1986)
Skåneprojektet - Hydrologisk och oceanografisk information för vattenplanering - Ett pilotprojekt.

5 Martin Häggström (1986)
Översiktlig sammanställning av den geografiska fördelningen av skador främst på dammar i samband med septemberflödet 1985.

6 Barbro Johansson (1986)
Vattenföringsberäkningar i Södermanlands län - ett försöksprojekt.

7 Maja Brandt (1986)
Areella snöstudier.

8 Bengt Carlsson, Sten Bergström, Maja Brandt och Göran Lindström (1987)
PULS-modellen: Struktur och tillämpningar.

9 Lennart Funkquist (1987)
Numerisk beräkning av vågor i kraftverksdammar.

10 Barbro Johansson, Magnus Persson, Enrique Aranibar and Robert Llobet (1987)
Application of the HBV model to Bolivian basins.

11 Cecilia Ambjörn, Enrique Aranibar and Roberto Llobet (1987)
Monthly streamflow simulation in Bolivian basins with a stochastic model.

12 Kurt Ehlert, Torbjörn Lindkvist och Todor Milanov (1987)
De svenska huvudvattendragens namn och mynningspunkter.

13 Göran Lindström (1987)
Analys av avrinningsserier för uppskattning av effektivt regn.

14 Maja Brandt, Sten Bergström, Marie Gardelin och Göran Lindström (1987)
Modellberäkning av extrem effektiv nederbörd.

15 Håkan Danielsson och Torbjörn Lindkvist (1987)
Sjökarte- och sjöuppgifter. Register 1987.

16 Martin Häggström och Magnus Persson (1987)
Utvärdering av 1986 års vårflödesprognoser.

17 Bertil Eriksson, Barbro Johansson, Katarina Losjö och Haldo Vedin (1987) Skogsskador - klimat.

18 Maja Brandt (1987) Bestämning av optimalt klimatstationsnät för hydrologiska prognoser.

19 Martin Häggström och Magnus Persson (1988) Utvärdering av 1987 års vårflödes-prognoser.

20 Todor Milanov (1988) Frysförluster av vatten.

21 Martin Häggström, Göran Lindström, Luz Amelia Sandoval and Maria Elvira Vega (1988) Application of the HBV model to the upper Río Cauca basin.

22 Mats Moberg och Maja Brandt (1988) Snökartläggning med satellitdata i Kultsjöns avrinningsområde.

23 Martin Gotthardsson och Sten Lindell (1989) Hydrologiska stationsnät 1989. Svenskt Vattenarkiv.

24 Martin Häggström, Göran Lindström, Luz Amelia Sandoval y Maria Elvira Vega (1989) Aplicacion del modelo HBV a la cuenca superior del Río Cauca.

25 Gun Zachrisson (1989) Svåra islossningar i Torneälven. Förslag till skadeförebyggande åtgärder.

26 Martin Häggström (1989) Anpassning av HBV-modellen till Torne-älven.

27 Martin Häggström and Göran Lindström (1990) Application of the HBV model for flood forecasting in six Central American rivers.

28 Sten Bergström (1990) Parametervärden för HBV-modellen i Sverige. Erfarenheter från modellkalibreringar under perioden 1975 - 1989.

29 Urban Svensson och Ingemar Holmström (1990) Spridningsstudier i Glan.

30 Torbjörn Jutman (1991) Analys av avrinningens trender i Sverige.

31 Mercedes Rodriguez, Barbro Johansson, Göran Lindström, Eduardo Planos y Alfredo Remont (1991) Aplicacion del modelo HBV a la cuenca del Río Cauto en Cuba.

32 Erik Arnér (1991) Simulering av vårflöden med HBV-modellen.

33 Maja Brandt (1991) Snömätning med georadar och snötaxeringar i övre Luleälven.

34 Bent Göransson, Maja Brandt och Hans Bertil Wittgren (1991) Markläckage och vattendragstransport av kväve och fosfor i Roxen/Glan-systemet, Östergötland.

35 Ulf Ehlin och Per-Eric Ohlsson, VASO (1991) Utbyggd hydrologisk prognos- och varningstjänst. Rapport från studieresa i USA 1991-04-22--30.

36 Martin Gotthardsson, Pia Rystam och Sven-Erik Westman (1992) Hydrologiska stationsnät 1992/Hydrological network. Svenskt Vattenarkiv.

37 Maja Brandt (1992) Skogens inverkan på vattenbalansen.

38 Joakim Harlin, Göran Lindström, Mikael Sundby (SMHI) och Claes-Olof Brandesten (Vattenfall Hydropower AB) (1992) Känslighetsanalys av Flödeskommitténs riktlinjer för dimensionering av hel älv.

39 Sten Lindell (1993) Realtidsbestämning av arealnederbörd.

40 Svenskt Vattenarkiv (1995) Vattenföring i Sverige. Del 1. Vattendrag till Bottenviken.

41 Svenskt Vattenarkiv (1995) Vattenföring i Sverige. Del 2. Vattendrag till Bottenhavet.

42 Svenskt Vattenarkiv (1993)
Vattenföring i Sverige. Del 3. Vattendrag till Egentliga Östersjön.

43 Svenskt Vattenarkiv (1994)
Vattenföring i Sverige. Del 4. Vattendrag till Västerhavet.

44 Martin Häggström och Jörgen Sahlberg (1993)
Analys av snösmältningsförlopp.

45 Magnus Persson (1993)
Utnyttjande av temperaturens persistens vid beräkning av volymsprognoser med HBV-modellen.

46 Göran Lindström, Joakim Harlin och Judith Olofsson (1993)
Uppföljning av Flödeskommitténs riktlinjer.

47 Bengt Carlsson (1993)
Alkalinitets- och pH-förändringar i Ume-älven orsakade av minimitappning.

48 Håkan Sanner, Joakim Harlin and Magnus Persson (1994)
Application of the HBV model to the Upper Indus River for inflow forecasting to the Tarbela dam.

49 Maja Brandt, Torbjörn Jutman och Hans Alexandersson (1994)
Sveriges vattenbalans. Årsmedelvärden 1961 - 1990 av nederbörd, avdunstning och avrinning.

50 Svenskt Vattenarkiv (1994)
Avrinningsområden i Sverige. Del 3. Vattendrag till Egentliga Östersjön och Öresund.

51 Martin Gotthardsson (1994)
Svenskt Vattenarkiv. Översvämningskänsliga områden i Sverige.

52 Åsa Evremar (1994)
Avdunstningens höjdberoende i svenska fjällområden bestämd ur vattenbalans och med modellering.

53 Magnus Edström och Pia Rystam (1994)
FFO - Stationsnät för fältforsknings-områden 1994.

54 Zhang Xingnan (1994)
A comparative study of the HBV model and development of an automatic calibration scheme.

55 Svenskt Vattenarkiv (1994)
Svenskt dammregister - Södra Sverige.

56 Svenskt Vattenarkiv (1995)
Svenskt dammregister - Norra Sverige.

57 Martin Häggström (1994)
Snökartering i svenska fjällområdet med NOAA-satellitbilder.

58 Hans Bertil Wittgren (1995)
Kvävetransport till Slätbaken från Söder-köpingsåns avrinningsområde

59 Ola Pettersson (1995)
Vattenbalans för fältforskningsområden.

60 Barbro Johansson, Katarina Losjö, Nils Sjödin, Remigio Chikwanha and Joseph Merka (1995)
Assessment of surface water resources in the Manyame catchment - Zimbabwe.

61 Behzad Koucheki (1995)
Älvtemperaturers variationer i Sverige under en tioårsperiod.

62 Svenskt Vattenarkiv (1995)
Sänkta och torrlagda sjöar.

63 Malin Kanth (1995)
Hydrokemi i fältforskningsområden.

64 Mikael Sundby, Rikard Lidén , Nils Sjödin, Helmer Rodriguez, Enrique Aranibar (1995)
Hydrometeorological Monitoring and Modelling for Water Resources Develop-ment and Hydropower Optimisation in Bolivia.

65 Maja Brandt, Kurt Ehlert (1996)
Avrinningen från Sverige till omgivande hav.

66 Sten Lindell, Håkan Sanner, Irena Nikolushkina, Inita Stikute (1996)
Application of the integrated hydrological modelling system IHMS-HBV to pilot basin in Latvia

67 Sten Lindell, Bengt Carlsson, Håkan Sanner, Alvina Reihan, Rimma Vedom (1996)

Application of the integrated hydrological modelling system IHMS-HBV to pilot basin in Estonia

68 Sara Larsson, Rikard Lidén (1996)
Stationstäthet och hydrologiska prognoser.

69 Maja Brandt (1996)
Sedimenttransport i svenska vattendrag exempel från 1967-1994.

70 Svenskt Vattenarkiv (1996)
Avrinningsområden i Sverige. Del 4.
Vattendrag till Västerhavet.

71 Svenskt Vattenarkiv (1996)
Svenskt sjöregister. 2 delar

72 Sten Lindell, Lars O Ericsson, Håkan Sanner, Karin Göransson SMHI
Malgorzata Mierkiewicz , Andrzej Kadlubowski, IMGW (1997)
Integrated Hydrological Monitoring and Forecasting System for the Vistula River Basin. Final report.

73 Maja Brandt, Gun Grahn (1998)
Avdunstning och avrinningskoefficient i Sverige 1961-1990. Beräkningar med HBV-modellen.

74 Anna Eklund (1998)
Vattentemperaturer i sjöar, sommar och vinter - resultat från SMHIs mätningar.

75 Barbro Johansson, Magnus Edström, Katarina Losjö och Sten Bergström (1998)
Analys och beräkning av snösmältningsförlopp.

76 Anna Eklund (1998)
Istjocklek på sjöar.

77 Björn Bringfelt (1998)
An evapotranspiration model using SYNOP weather observations in the Penman-Monteith equation

78 Svenskt Vattenarkiv (1998)
Avrinningsområden i Sverige. Del 2
Vattendrag till Bottenhavet.

79 Maja Brandt, Anna Eklund (1999)
Snöns vatteninnehåll Modellberäkningar och statistik för Sverige

80 Bengt Carlsson (1999)
Some facts about the Torne and Kalix River Basins.
A contribution to the NEWBALTIC II workshop in Abisko June 1999.

81 Anna Eklund (1999)
Isläggning och islossning i svenska sjöar.

82 Svenskt Vattenarkiv (2000)
Avrinningsområden i Sverige. Del 1.
Vattendrag till Bottenviken.

83 Anna Eklund, Marie Gardelin, Anders Lindroth (2000)
Vinteravdunstning i HBV-modellen - jämförelse med mätdata

84 Göran Lindström, Mikael Ottosson Löfvenius (2000)
Tjäle och avrinning i Svartberget – studier med HBV-modellen

85 Bengt Carlsson och Göran Lindström (2001)
HBV-modellen och flödesprognoser

SMHI
Sveriges meteorologiska och hydrologiska institut
601 76 Norrköping
Tel 011-495 80 00 · Fax 011-495 80 01

ISSN 0283-7722